Netherlands
organization for
applied scientific
research

TNO-report

FEL

TNO Physics and Electronics
Laboratory

P.O. Box 96864
2509 JG The Hague
Oude Waalsdorperweg 63
The Hague, The Netherlands

Fax +31 70 328 09 61
Phone +31 70 326 42 21

1

report no.
FEL-91-B043

copy no.
2

title

Validation of diffraction theory by means of extensive measurements, part 1.

author(s):

Ir. J.F.A. Koppelmans

date :

April 1991

classification

title	: unclassified
abstract	: unclassified
report text	: unclassified
appendix A	: unclassified

no. of copies	: 21
no. of pages	: 69 (incl. appendix, excl. distr.list)
appendices	: 1

TNO

report no.	:	FEL-91-B043
title	:	Validation of diffraction theory by means of extensive measurements, part 1.
author(s)	:	Ir. J.F.A. Koppelmans
institute	:	TNO Physics and Electronics Laboratory
date	:	April 1991
NDRO no.	:	-
no. in pow '91	:	710.5
Research supervised by:		Ir. H.J.M. Heemskerk
Research carried out by:		Ir. J.F.A. Koppelmans

ABSTRACT (UNCLASSIFIED)

In the FEL computer model the radar cross section of arbitrary objects is calculated by applying geometrical optics and physical optics. In order to perform the computations more accurately, the model also accounts for diffraction phenomena. This report presents a large number of measurements and simulations carried out to validate the diffraction theory implemented.

During the analysis of the results, it turned out that there was a large difference between measurements using horizontal polarization and those using vertical polarization. At vertical polarization the measurements and simulations generally showed good agreement. At horizontal polarization, however, large differences between the measurements and the simulations occurred. Further analysis showed that these differences were most likely due to the fact that the implemented diffraction theory does not account for multiple diffraction. Apart from that, the anechoic chamber caused problems because of its relatively high "clutter level", which was in the same order of magnitude as the measured signals.

For further validation efforts, it is therefore recommended to include multiple diffraction in the computer model and to perform new measurements under better controlled circumstances.

rapport no.	:	FEL-91-B043
titel	:	Validatie van een diffractietheorie door middel van een groot aantal metingen deel 1.
auteur(s)	:	Ir. J.F.A. Koppelmans
instituut	:	Fysisch en Elektronisch Laboratorium TNO
datum	:	april 1991
hdo-opdr.no.	:	-
no. in iwp '91	:	710.5
Onderzoek uitgevoerd o.l.v.	:	Ir. H.J.M. Heemskerk
Onderzoek uitgevoerd door	:	Ir. J.F.A. Koppelmans

SAMENVATTING (ONGERUBRICEERD)

Het FEL computer model maakt gebruik van geometrische optica en fysische optica voor het berekenen van de radardoorsnede van willekeurige voorwerpen. Om deze berekeningen nauwkeuriger te kunnen uitvoeren, zijn ook diffractieverschijnselen in het model opgenomen. Dit rapport beschrijft een groot aantal metingen en simulaties, die zijn uitgevoerd ter validatie van de geimplementeerde diffractietheorie.

Bij de analyse van de resultaten bleek, dat er een duidelijk onderscheid moest worden gemaakt tussen metingen met horizontale polarisatie en die met vertikale polarisatie. In het geval van vertikale polarisatie kwamen de metingen en de simulaties over het algemeen vrij goed overeen. Bij horizontale polarisatie traden echter grote verschillen op. Nadere analyses hebben aangetoond, dat deze verschillen waarschijnlijk veroorzaakt worden door het niet meenemen van meervoudige diffractie-verschijnselen in het computermodel. Daarnaast veroorzaakte de reflectie-arme kamer problemen, doordat zijn "clutter niveau" in de zelfde orde van grootte lag als de te meten signalen.

Bij verdere validaties is het daarom aan te bevelen meervoudige diffractie in het computermodel te verwerken en nieuwe metingen uit te voeren onder beter geconditioneerde omstandigheden.

1 INTRODUCTION

In the past few years, the millimeterwave section of the radar group at FEL-TNO has made a great effort in developing a computer program capable of calculating the radar cross section (RCS) of arbitrary objects. To do so, the object has to be modelled by a number of polygons. By applying Geometrical Optics (GO) and Physical Optics (PO), the RCS of the object can be estimated. This was done in the first version of the RCS program [1]. Physical Optics is a method of approximating the electromagnetic field scattered by a flat plate much larger than the wavelength λ. It does, however, not account for the diffraction phenomena occurring at the edge of the plate. Therefore the program was extended with diffraction theory as described in [2]. This second version of the RCS program thus combines Geometrical Optics, Physical Optics and diffraction theory.

This report presents a number of measurements which where carried out in order to validate the implemented diffraction theory. The RCS of a total of six different objects are both measured and computed and the results are compared.

The second chapter of the report deals with the measurement principle and setup. The measurement results are discussed in chapter three.

2 MEASUREMENT PRINCIPLE

2.1 Measurement setup

The block diagram of the measurement setup is shown in figure 1a.

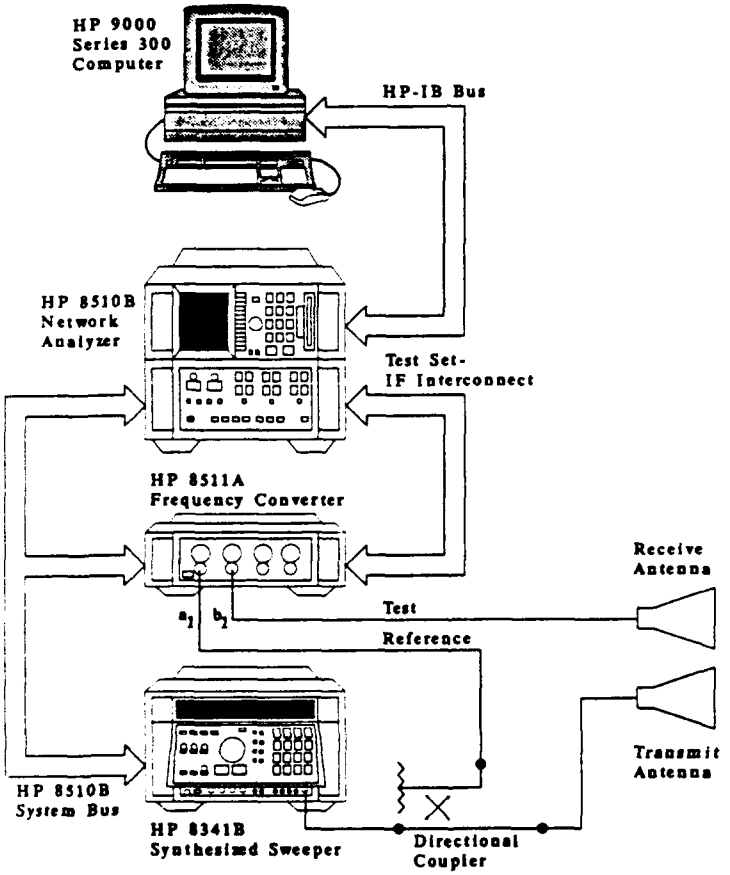

Fig. 1a: The measurement setup.

The measurements are controlled by a HP9000 series 300 computer. The computer is connected to a HP8510B network analyser via a HP-IB interface. To start a measurement, the computer gives a number of instructions to the network analyser. Then the network analyser takes over control of the actual measurement, steering the signal source (a HP8341B synthesized sweeper) and the HP8511A frequency converter via the HP8510B system bus. The output of the signal source is connected to the transmit antenna via a directional coupler. Part of the transmit signal is

coupled into the a1 input of the frequency converter to serve as a reference signal for the network analyser. The transmit antenna is mounted at the end of an anechoic chamber (see figure 1b). The test object is placed on a pedestal in the middle of the chamber at a distance of about 3.5 m from the antenna. Part of the transmitted signal is reflected by the test object and received by a second antenna mounted next to the transmit antenna. The signal from this receive antenna is fed into the b1 input of the frequency converter. In the frequency converter, a1 and b1 are converted to an intermediate frequency and then output to the network analyser for further analysis. The results of this analysis are transferred back to the computer and stored on a floppy disk.

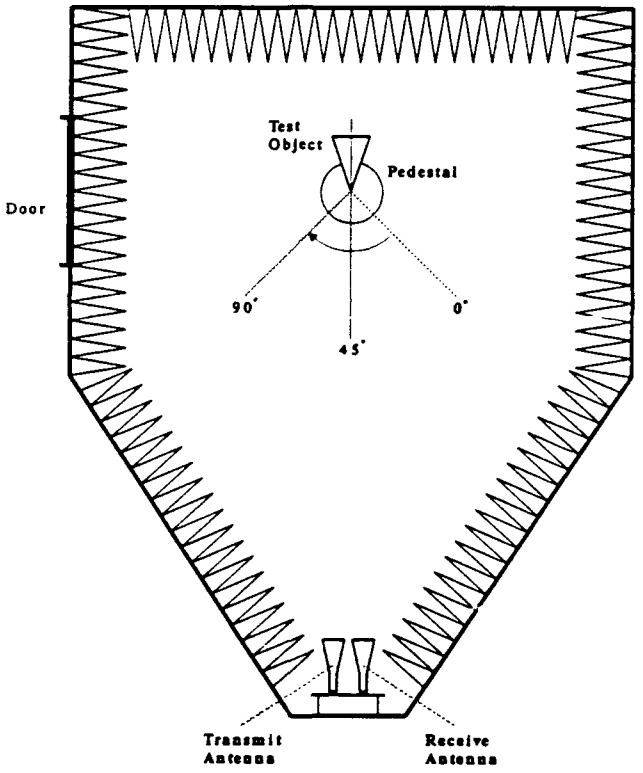

Fig. 1b: Positioning of the transmit and receive antennas and the test object.

2.2 Measurement principle

When measuring radar cross sections, a number of problems arise. The main ones are :

- noise
- reflections in the anechoic chamber
- leakage between transmit and receive antenna.

The solution to these problems is threefold, namely :

- averaging
- calibration
- time gating.

The easiest way to reduce the effects of noise, is to perform each measurement a number of times and to average the results. To limit the measurement time, an averaging factor of 128 has been used. This decreases the noise level by 10Ølog(128) = 21.1 dB.

The best way to compensate for the reflections of the anechoic chamber and the antenna crosstalk is to perform a calibration. The calibration procedure is as follows :

1: measure the (known) maximum RCS of a reference object as function of the frequency (trace 1)
2: measure the RCS of the empty chamber as function of the frequency (trace 2)
3: subtract trace 2 from trace 1 to obtain the corrected response of the reference object (trace 3); trace 2 and 3 form the calibration file
4: subtract trace 2 from the measurement results of the test object to compensate for unwanted reflections and antenna crosstalk; compare the result with trace 3 to get the RCS in dBsqm.

Calibration has to be performed separately for horizontal and vertical polarization, because the chamber characteristics depend on the polarization. It should also be noted, that after calibration the 0 dB level corresponds to the RCS of the reference object and that the maximum of the reflection of the testobject lies at t=0 if the location of the testobject is the same as for the reference object.

The last technique mentioned above is time gating. This is a method to further reduce the unwanted signals remaining after calibration. The method works as follows :

1: compute the inverse Fourier transform of the received signal (from frequency to time domain)
2: put a time gate (a time bandpass filter) around the center of the wanted scatterer: note that scatterers with different pathlengths get different time delays
3: compute the Fourier transform of the time filtered signal to get the frequency response of the test object.

Time gating is primarily used to reduce the unwanted signals remaining after calibration, but can also reduce the effects of multipath, provided that the socalled alias free range is large enough. The alias free range is the distance in the time domain at which periodic repetitions (aliasing) of the response occur. This periodicity is caused by performing the frequency domain measurements at discrete equidistant frequencies. The spacing between the repetitions is the reciproke of the frequency spacing of the samples. In our case, the frequency band is 2 GHz wide (16-18 GHz). When the number of frequency points is set to 101, the frequency spacing becomes 20 MHz. For reflection measurements this gives an alias free range of 7.5 m. Due to the applied time window the range resolution is 15 cm. In this way, multipath effects can be effectively cancelled. The optimum gate span of the time filter was empirically found to be 4 ns.

By combining the above described techniques (averaging, calibration and time gating), the total "clutter" level of the measurement setup was brought to an acceptable level. This was checked by measuring the RCS of the empty chamber. The results are shown in figures 2-7 for horizontal and vertical polarization at 16, 17 and 18 GHz. The average clutter levels in dBm are given in table 1.

Frequency:	16 GHz	17 GHz	18 GHz
Horizontal pol.	-29.1	-30.1	-29.4
Vertical pol.	-31.8	-30.5	-26.7

Table 1: Average "clutter levels" of the anechoic chamber in dBm .

It can be seen from table 1 that the anechoic chamber performs better for vertical then for horizontal polarization at 16 and 17 GHz, but at 18 GHz the reverse is true. Furthermore, the 17 GHz figures indicate that the anechoic chamber is somewhat asymmetrical, performing better in the right part. Finally, two more things should be noted, namely :

- during all measurements and simulations, the pedestal was rotated from 0° to 90° in steps of 1°, with the point of symmetry lying at 45° (see figure 1b).
- an aluminium plate of 20 x 20 cm was used as reference object; the theoretical RCS of this plate is :

  57.2 m = 17.6 dBm at 16 GHz
  64.6 m = 18.1 dBm at 17 GHz
  72.4 m = 18.6 dBm at 18 GHz.

To check if the calibrations were performed correctly, the RCS of a trihedral corner reflector was both measured and computed. The results are shown in figures 8-13 for horizontal and vertical polarization at 16, 17 and 18 Ghz. From these figures it can be seen that the maximum difference (computed RCS at 45° - measured RCS at 45°) varies from -2.5 to +0.5 dB. For this difference there are four possible causes. These are:

- changes in the chamber characteristics due to its poor mechanical condition
- imperfections of the corner reflector
- the narrow beamwidth of the reference plate (2.2°) causing positioning difficulties and hence a too large measured RCS of the test object
- the bistatic angle (1.4°) of the test setup, which was not accounted for in the simulations; this could cause a difference of -1.13 dB.

2.3 Measurement objects

In order to validate the implemented diffraction theory, five different objects were used, namely four wedges and a plate. This was done because the implemented theory distinguishes between wedge sides and knife sides (a knife is a wedge with an exterior angle of 360°). The ideal object to validate the "knife diffraction" would be an infinetely thin plate with a perfectly conducting surface. Perfect conductivity is required because of assumptions made in the theory. This ideal object was approached by a 10 x 10 cm copper plate, 0.6 mm thick. To approach perfect conductivity, the surface of the plate was covered with 10 microns of silver (the skindepth is about ½ micron in the 16-18 GHz frequency range). The four wedges were made of massive aluminium with a silvered surface. The two sides enclosing the interior wedge angle were 10 x 10 cm large and the four wedge angles used were 5°, 10°, 20° and 45°. From now on, these wedges will be denoted Wg05, Wg10, Wg20 and Wg45 respectively.

3 SIMULATIONS AND MEASUREMENTS

3.1 Introduction

This chapter presents the results of a large number of simulations and measurements. Although the simulations and measurements are treated separately, corresponding results (figures) are printed on the same page. This is done for comparative purposes.

3.2 Simulations

All simulations were carried out using the ANAL2.F program [3]. The program was run on a Convex C220 minisupercomputer. For each run, three input files were required, namely:

- a file 'MATERIALS' containing the material parameters
- a file 'OBJECT' containing a model of the testobject
- a file 'PARAMETERS' containing the simulation parameters.

The MATERIALS file [4] contains the reflection coefficients of a few materials for a number of angles of incidence.

For each of the six objects used (five testobjects and the corner) an OBJECT file was created using the SCARCE.F program [5]. The contents of these files are listed in appendix A. To control the simulations six PARAMETERS files were used, namely for horizontal and vertical polarization at 16, 17 and 18 GHz. These files are also listed in appendix A. By combining six object files with six parameter files, a total of 36 simulations is obtained. The results of the simulations were transferred from the Convex C220 to a PC (under MS-DOS) for further processing. This processing was done using the HARVARD GRAPHICS package, which resulted in the top figures of figure 8-43. The title above each figure indicates the object, the frequency and the polarization used.

3.3 Measurements and dataprocessing

All measurements were performed using the test setup described in chapter 2. As mentioned earlier, the measurements were controlled by a HP9000 series 300 computer and the results were stored on 3½" floppy disks within this computer. In order to be able to use HARVARD for the data processing, the data had to be converted from HP to MS-DOS format. This was necessary

because HP uses a proprietary disk format which is not compatible with MS-DOS. The conversion was done using the HPDOS.EXE program [6]. The output of the converter, however, was not suitable to be imported into HARVARD. Therefore, a kind of Harvard PreProcessor called HPP.PAS was written. This program rearranged the converted data and corrected it for the computed RCS of the reference object (see section 2.2). The output of HPP was then processed using HARVARD, giving the bottom figures of figure 8-43.

3.4 Results

The results of the simulations and measurements presented in figure 8-43 contain such an amount of detail that it would be very tedious to deal with each figure separately. Therefore, it was decided to select a number of criteria and to apply them to each simulation/measurement pair. By representing the outcome of these applications using a matrix form, general characteristics can easily be tracked down. The criteria chosen were:

- the overall shape of the figure
- the shape of the left part of the figure
- the shape of the right part of the figure
- the RCS at an angle of 45°
- the average RCS level

To simplify comparison of the results, three small matrices are used instead of one large one, namely for 16, 17 and 18 GHz. The top half of each matrix gives the results for horizontal polarization and the bottom half for vertical polarization. The three matrices are shown in tables 2-4.

Column 1-3 of tables 2-4 use the following notation:

++ : shapes match very well
+ : shapes match well
Ø : shapes match resonably
- : shapes match badly
-- : shapes match very badly

Column 4 lists the computed RCS at 45° minus the measured RCS at 45° and column five lists the computed average RCS minus the measured average RCS.

Object	Overall shape	Left shape	Right shape	ΔRCS at 45°	Δaverage RCS
Corn H	++	++	+	0.5	-1.0
Plt H	--	--	-	?	-1.7
Wg05 H	-	-	--	7.0	-0.5
Wg10 H	--	--	--	14.0	-0.9
Wg20 H	--	--	--	6.0	-0.5
Wg45 H	+	+	Ø	-2.0	0.3
Corn V	+	+	Ø	0.5	-0.6
Plt V	+	+	++	-2.0	-3.7
Wg05 V	+	+	Ø	0.5	-0.5
Wg10 V	+	+	Ø	0.5	-0.6
Wg20 V	+	+	Ø	0.5	-0.6
Wg45 V	+	+	+	-1.0	-0.8

Table 2: Summary of the simulation/measurement results at 16 GHz.

Object	Overall shape	Left shape	Right shape	ΔRCS at 45°	Δaverage RCS
Corn H	++	++	++	-1.5	-1.5
Plt H	--	--	-	?	-1.6
Wg05 H	-	-	Ø	6.0	-1.1
Wg10 H	--	--	-	13.0	-1.4
Wg20 H	--	-	Ø	6.0	-1.5
Wg45 H	+	+	+	-2.0	0.6
Corn V	+	+	Ø	-1.0	-1.2
Plt V	+	+	++	-3.5	-4.4
Wg05 V	+	+	Ø	0.0	-0.0
Wg10 V	+	+	Ø	0.5	-0.3
Wg20 V	+	+	Ø	-0.5	-0.1
Wg45 V	++	+	++	1.5	-0.8

Table 3: Summary of the simulation/measurement results at 17 GHz.

It should be noted that the evaluation of the figures is somewhat subjective except for the average RCS. By comparison of the three matrices we can draw the following conclusions with respect to the five applied criteria :

Overall shape

- At horizontal polarization, only the corner and Wg45 give good results. As can be seen in figures 8, 9 and 10, the simulations and measurements of the corner match very well. Wg45 shows also good agreement between the measurements and the simulations, but this is7 mainly the result of the large contribution of PO with respect to that of the diffraction on the wedge. This is due to the increase of the angle of incidence on the plates forming the wedge as the wedge angle increases. The plate and the three smallest wedges give rather poor results, which will be discussed in a more detailed manner in section 3.5.

Object	Overall shape	Left shape	Right shape	ΔRCS at 45°	Δaverage RCS
Corn H	++	+	++	-2.0	-1.6
Plt H	-	-	-	?	-2.0
Wg05 H	--	--	-	10.0	-2.1
Wg10 H	--	--	--	10.0	-2.6
Wg20 H	Ø	Ø	Ø	2.0	-2.9
Wg45 H	+	+	+	-5.0	2.1
Corn V	+	+	Ø	-2.5	-1.5
Plt V	-	-	-	2.0	0.1
Wg05 V	+	+	++	-2.0	-4.5
Wg10 V	+	Ø	+	-2.0	-4.5
Wg20 V	+	Ø	+	-1.5	-4.3
Wg45 V	+	+	++	2.0	-3.8

Table 4: Summary of the simulation/measurement results at 18 GHz.

- When using vertical polarization, all measurements give good or very good results, except for the plate (Plt) at 18 GHz. Because the error occurs only at 18 GHz it is most likely caused by somekind of interference problem.
- Although, generally spoken, measurements using vertical polarization give much better results than those using horizontal polarization, the corner performs best at horizontal polarization. The only reasonable explanation for this is that the corner was not correctly positioned in the anechoic chamber during the vertical measurements.

Left versus right shapes

- At 16 GHz the left part of most figures matches better than the right part.
- At 17 and 18 GHz the right part of most figures matches better.
- In 8 of the 36 measurements the result is symmetric in the sence that the left and the right part of the figure are judged equally.

RCS at 45°

- When horizontal polarization is considered, it turns out that the computed RCS at 45° of the three smallest wedges at all frequencies is larger than the measured RCS. This is caused by the fact that the peaks of the RCS around 45° occurring in the simulations do not occur in the measurements. This is most likely caused by an imperfection in the diffraction theory implemented (see also section 3.5). The largest wedge shows reasonable agreement between the simulations and measurements due to the relative large contribution of PO. In case of the plate, the simulations show a near zero RCS at 45°, which is also found in the measuments. Note, however, that the depth of the null in the measurements is limited by the environment whereas in the simulations it is unlimited.
- At vertical polarization there is a notable difference in the agreement between the measurements/simulations at 16 and 17 GHz and those at 18 GHz. At 16 and 17 GHz the computed RCS at 45° of the corner and the wedges shows good agreement with the measurements. The plate gives poorer results, most likely due to its smaller reflections. At 18 GHz, however, none of the testobjects gives good results. This has probably got something to do with the relatively high reflections of the anechoic chamber under these conditions (see table 1, section 2.2).

Average RCS

- First consider horizontal polarization. At 16 and 17 GHz all measured average RCSs lay within 1.7 dB from the computed average RCSs. It should be noted that only in one case (Wg45 at 16 GHz) the measured average RCS is smaller than the computed average RCS. In all other cases, the measured average RCS is 0.5 to 1.7 dB too large, which is in good agreement with the RCS difference analysis of section 2.2. At 18 GHz all measurements show an average RCS which is 1.6 to 2.9 dB too large. This cannot be explained by the clutter levels of the anechoic chamber but is the result of alignment errors of the reference plate giving too large measured RCSs like before.

- When considering vertical polarization the same separation between 16/17 and 18 GHz can be made. At 16 and 17 GHz all testobjects except the plate have a computed average RCS within 1.2 dB from the measured average RCS. Like before, the measured average RCS is usually too large. In the case of the plate the shape of the measured figures matches well with the simulations, but the average level is at about 4 dB too high. At 18 GHz the high clutter level of the anechoic chamber causes the measured average RCSs of all four wedges to be circa 4 dB too large. The corner suffers less from this phenomenon (average RCS 1.5 dB too large) because of its stronger reflections. Finally, in case of the plate, we find an almost ideal average RCS; but this seems just a lucky coincidence because the shapes of the measured and simulated figures match badly (compared to those at 16 and 17 GHz).

3.5 Further analysis

In the previous section it turned out that the measurements/simulations using vertical polarization match much better than those using horizontal polarization. Because the measurement conditions are almost equal for both polarizations, the cause for this must be searched for in the simulation results using horizontal polarization.

The most likely cause for the discrepancies is indicated by Ross [7], who states that it is necessary to include multiple diffraction terms in order to account for the polarization dependence of radar cross sections. The diffraction model as described in [2] does however not account for multiple diffraction. After studying some additional literature it turned out to be impossible to include multiple diffraction in the RCS program in a simple and elegant way. The only testobject for which the RCS including multiple diffraction can be computed quite easily is the plate. Bowman [8] gives the total diffracted field of an infinite strip of width d. By combining Bowman's results for the infinite strip with the incremental diffraction coefficients for planar surfaces of Shore and Yaghjian [9] the field scattered by a finite strip (thus a plate) can be computed. The results are shown as the solid lines in the top figures of figure 44-49 for horizontal and vertical polarization at 16, 17 and 18 GHz. The corresponding measurements are shown at the bottom of the figures.

When studying figures 44-49, it should be noted that Bowman's results are not valid for observation angles near grazing incidence. In our case this means between circa 40 and 50 degrees. Ross has shown that the dashed lines in figures 44-49 apply in this angle interval. Taking this into account, and comparing figures 44-49 with figures 14-19, we can conclude that

Bowman's results match much better with the measurements than the original simulations. The differences between the new simulations and the measurements remain, however, still quite large. Nevertheless, it seems very likely that multiple diffraction has a substantial influence on radar cross sections. Figures 44-49 also show that multiple diffraction has a much larger influence at horizontal polarization than at vertical polarization. This can be explained as follows: For a vertical plate and horizontal polarization the E-vector of the incident electromagnetic field can be decomposed into a component perpendicular to the plate and a component parallel to the plate (from front to back). This last component induces surface currents between the front and rear end of the plate. These currents exite radiation fields, which contribute directly to the total scattered field. For a vertical plate and vertical polarization the E-vector of the incident field is directed parallel to the plate (from bottom to top). The surface currents induced by this field do, however, not give rise to a scattered field in the direction of incidence.

To study the influence of multiple diffraction phenomena in more detail, it is recommended to modify the RCS program such that it can account for multiple diffraction of arbitrary objects and then applying it to the wedges.

4 DISCUSSION

Based on the measurements and simulations treated in the previous sections, we can draw the following conclusions with respect to the implemented diffraction theory:

- at vertical polarization, the measurements and simulations show good agreement and thus the diffraction theory is thought to be correctly implemented.
- at horizontal polarization, there is only little agreement between the measurements and the simulations. The cause of this is most probably the fact that multiple diffraction phenomena are not accounted for in the current computer model.

It should be noted that both horizontal and vertical measurements suffer from the relatively high "clutter level" of the anechoic chamber, causing large disturbances and thus uncertainties of the measured signal. For further validation efforts it is therefore recommended to:

- perform new simulations for horizontal polarization using a computer model which includes multiple diffraction.
- perform new measurements for both polarizations under better controlled circumstances, that is in an anechoic chamber with a lower clutter level.

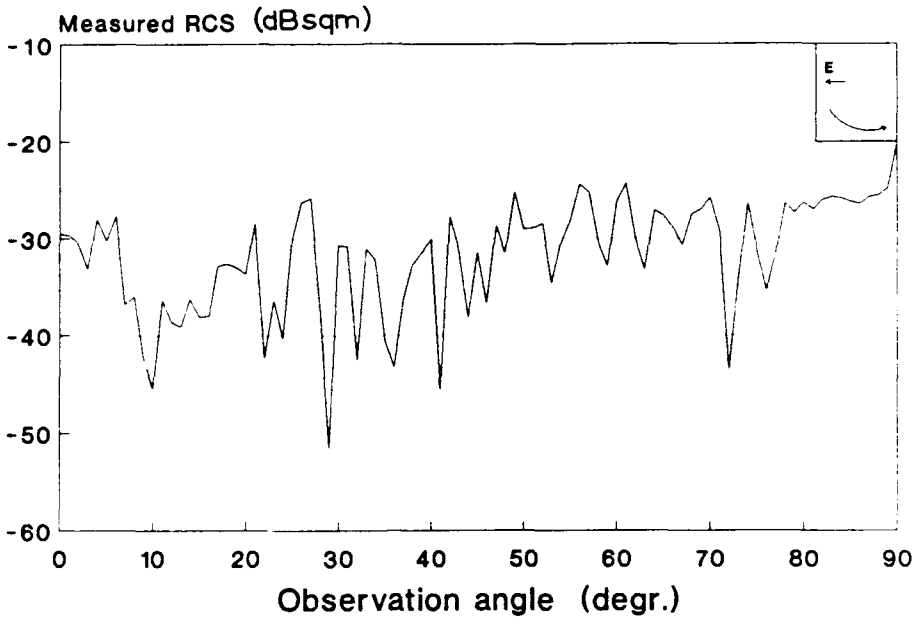

Fig. 2: Measured RCS of the anechoic chamber at 16 GHz and horizontal polarization.

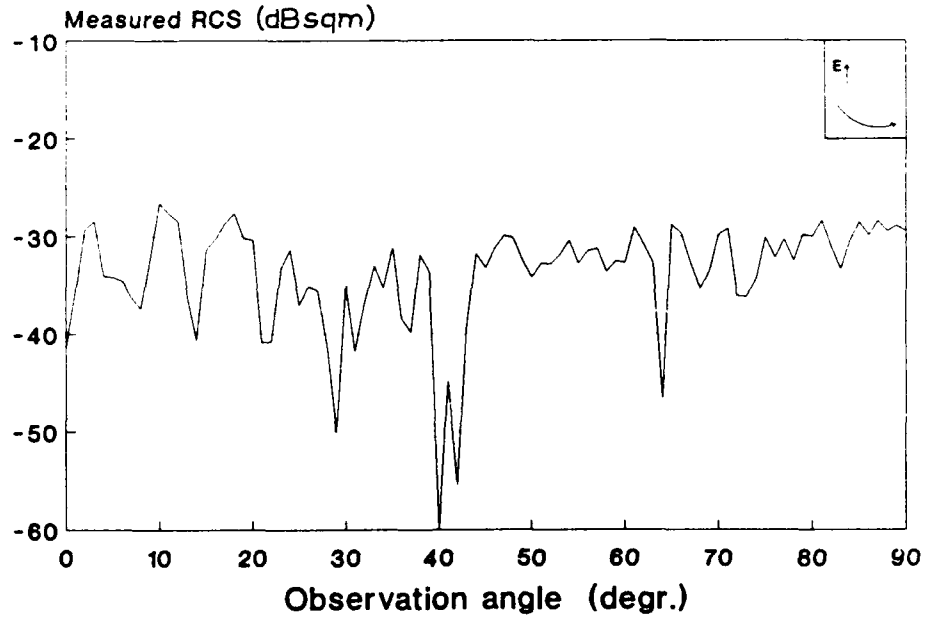

Fig. 3: Measured RCS of the anechoic chamber at 16 GHz and vertical polarization.

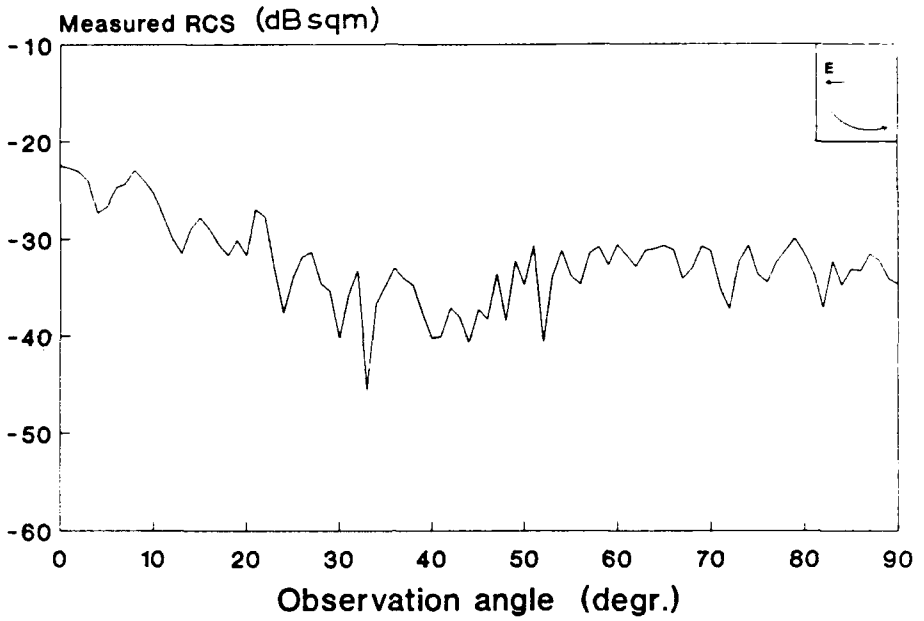

Fig. 4: Measured RCS of the anechoic chamber at 17 GHz and horizontal polarization.

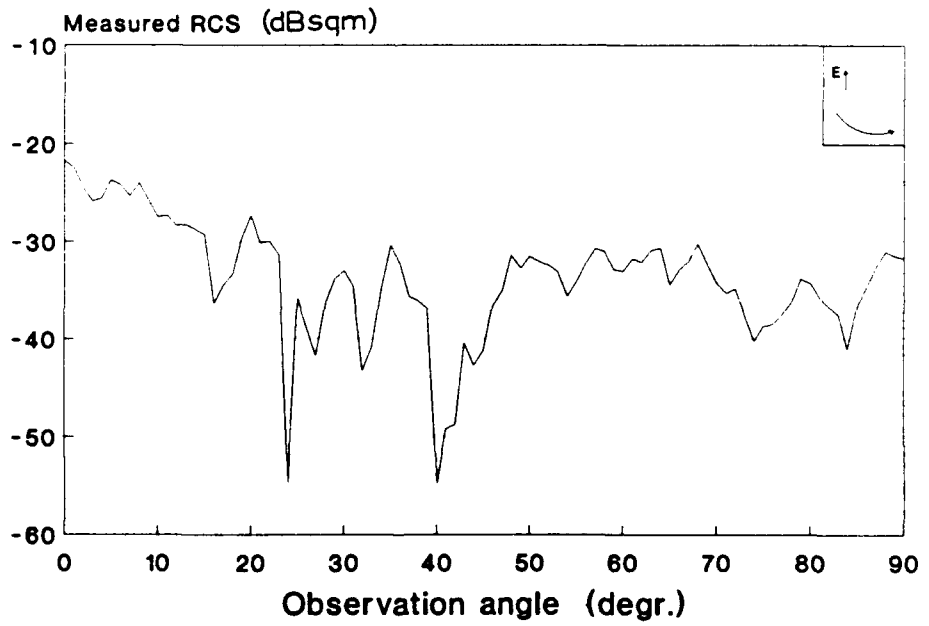

Fig. 5: Measured RCS of the anechoic chamber at 17 GHz and vertical polarization.

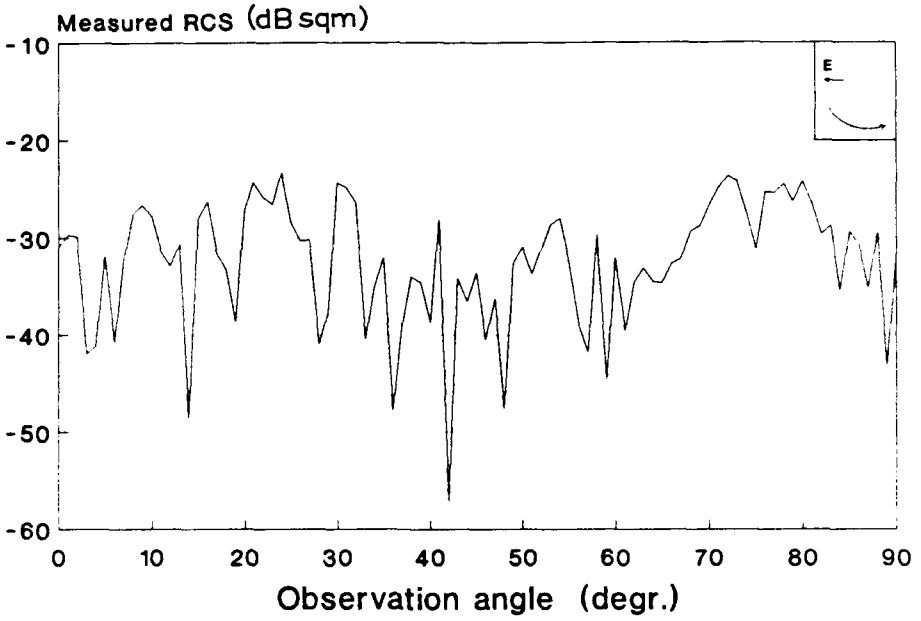

Fig. 6: Measured RCS of the anechoic chamber at 18 GHz and horizontal polarization.

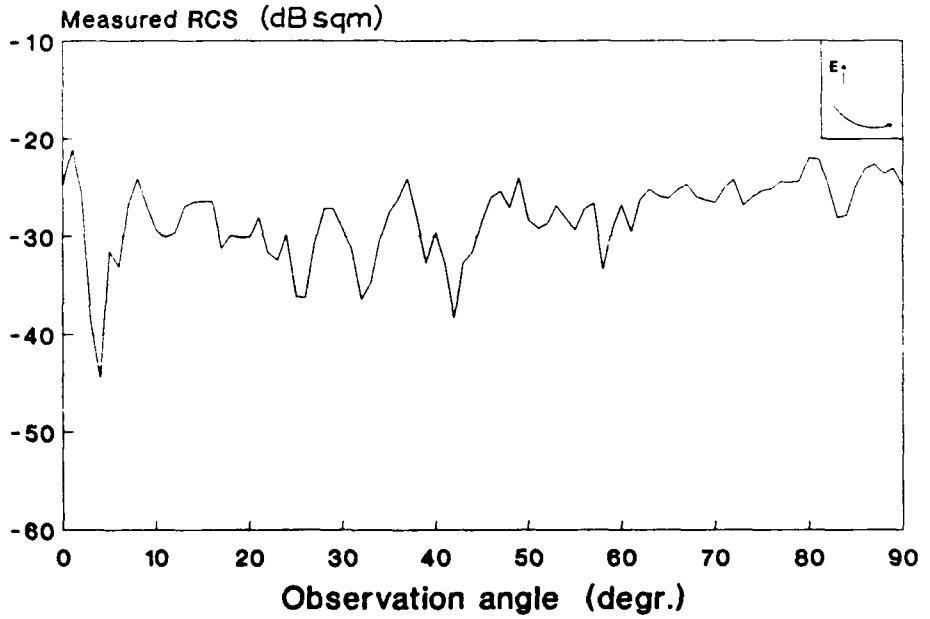

Fig. 7: Measured RCS of the anechoic chamber at 18 GHz and vertical polarization.

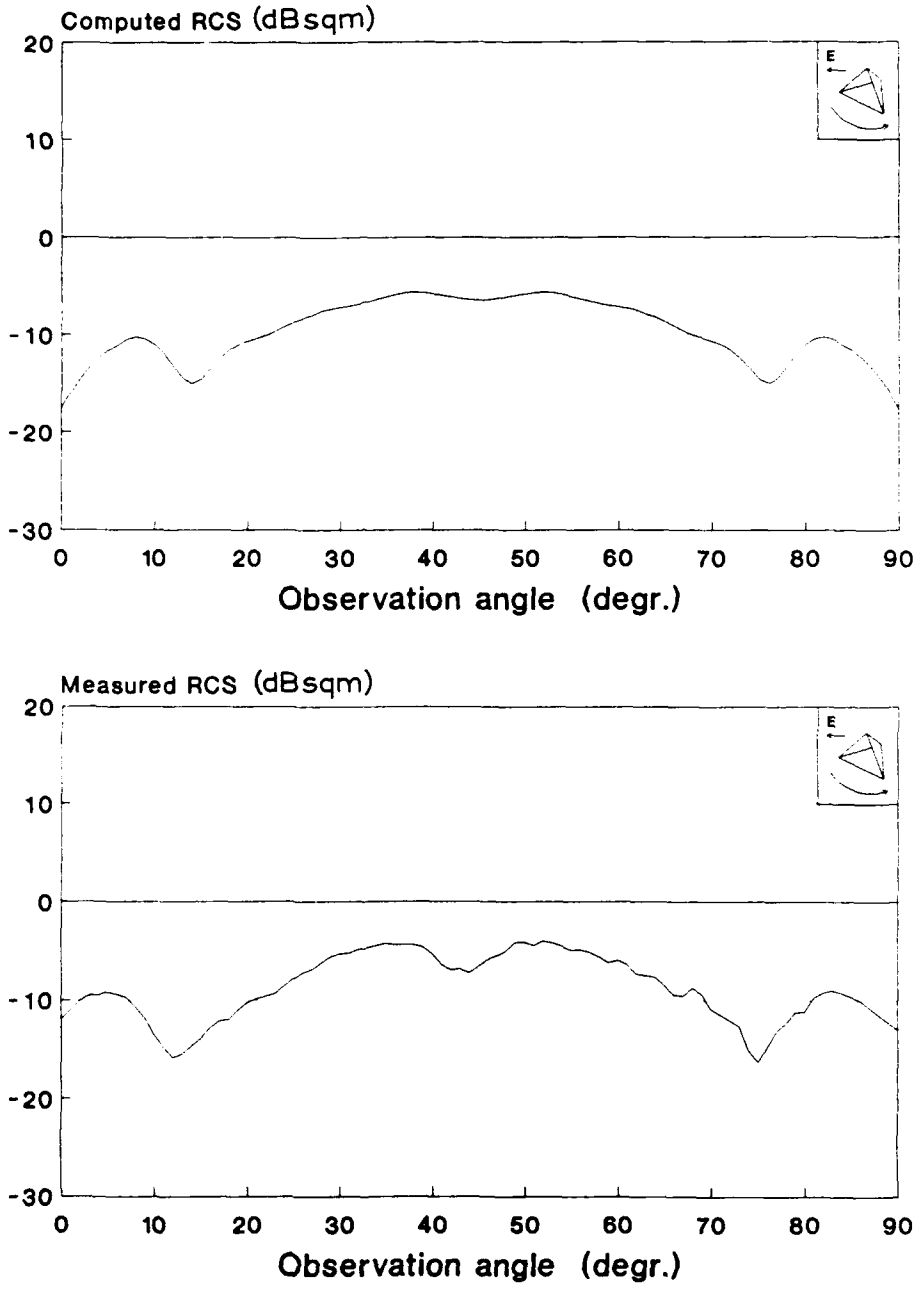

Fig. 8: Computed and measured RCS of the corner reflector at 16 GHz and horizontal polarization.

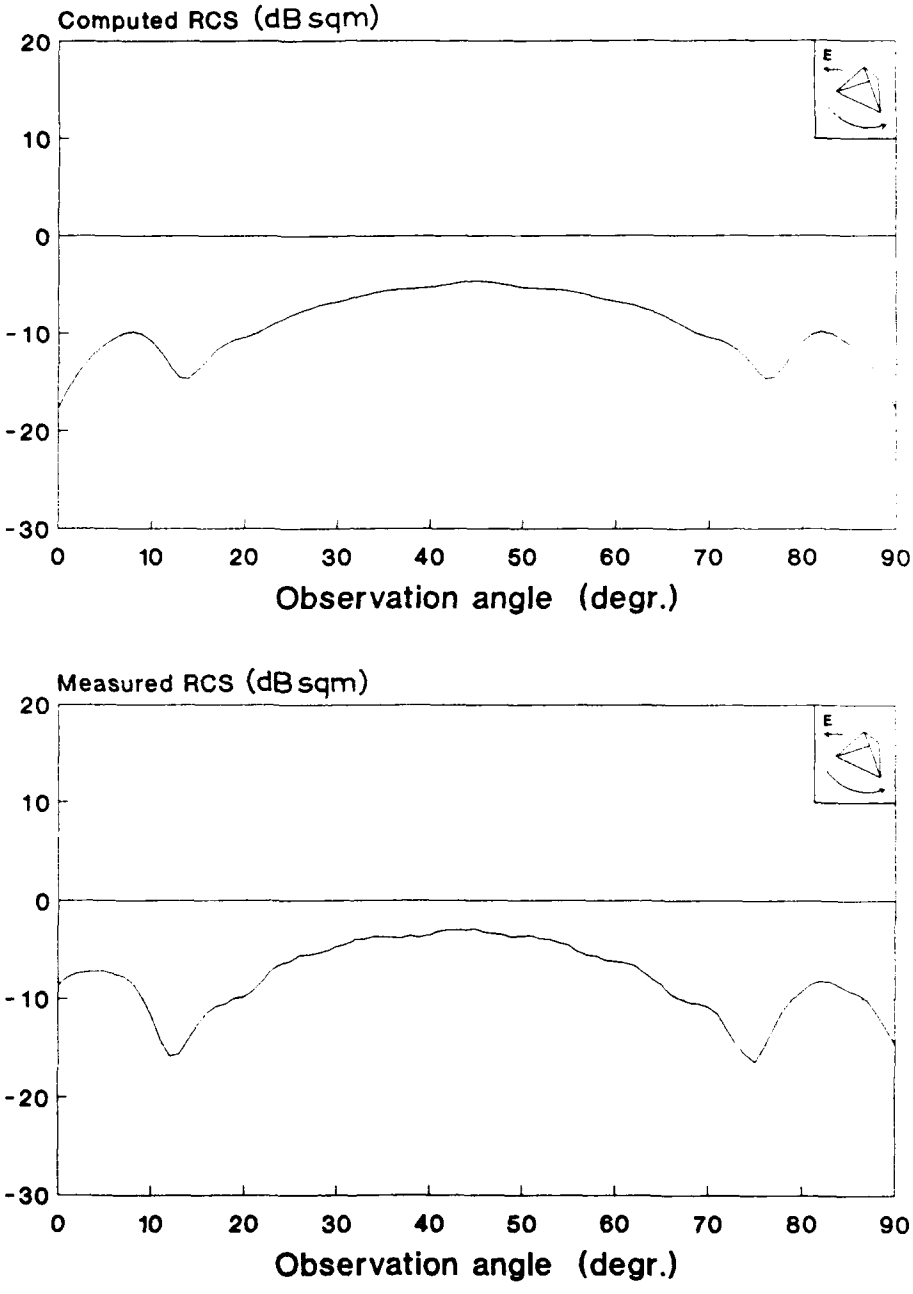

Fig. 9: Computed and measured RCS of the corner reflector at 17 GHz and horizontal polarization.

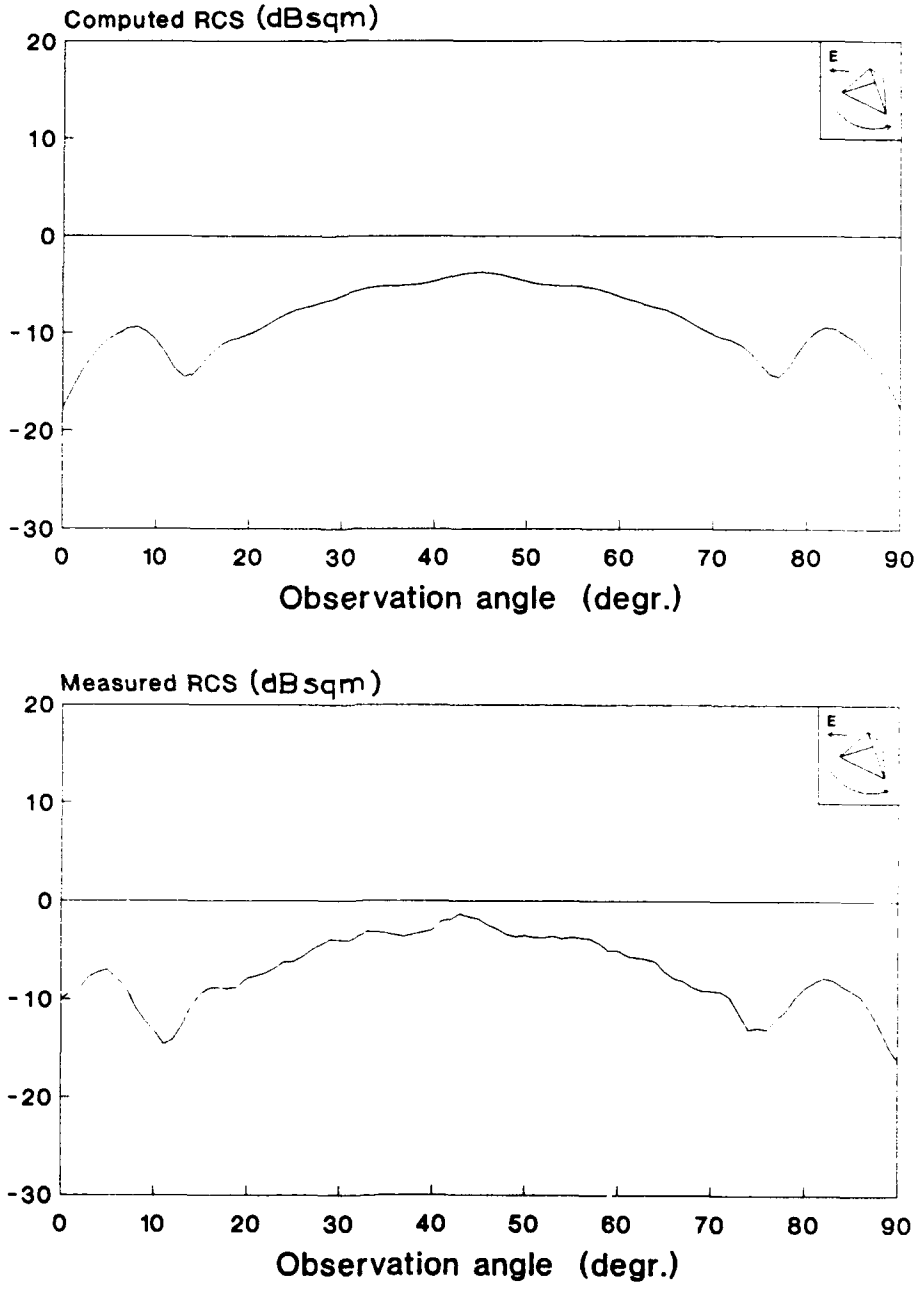

Fig. 10: Computed and measured RCS of the corner reflector at 18 GHz and horizontal polarization.

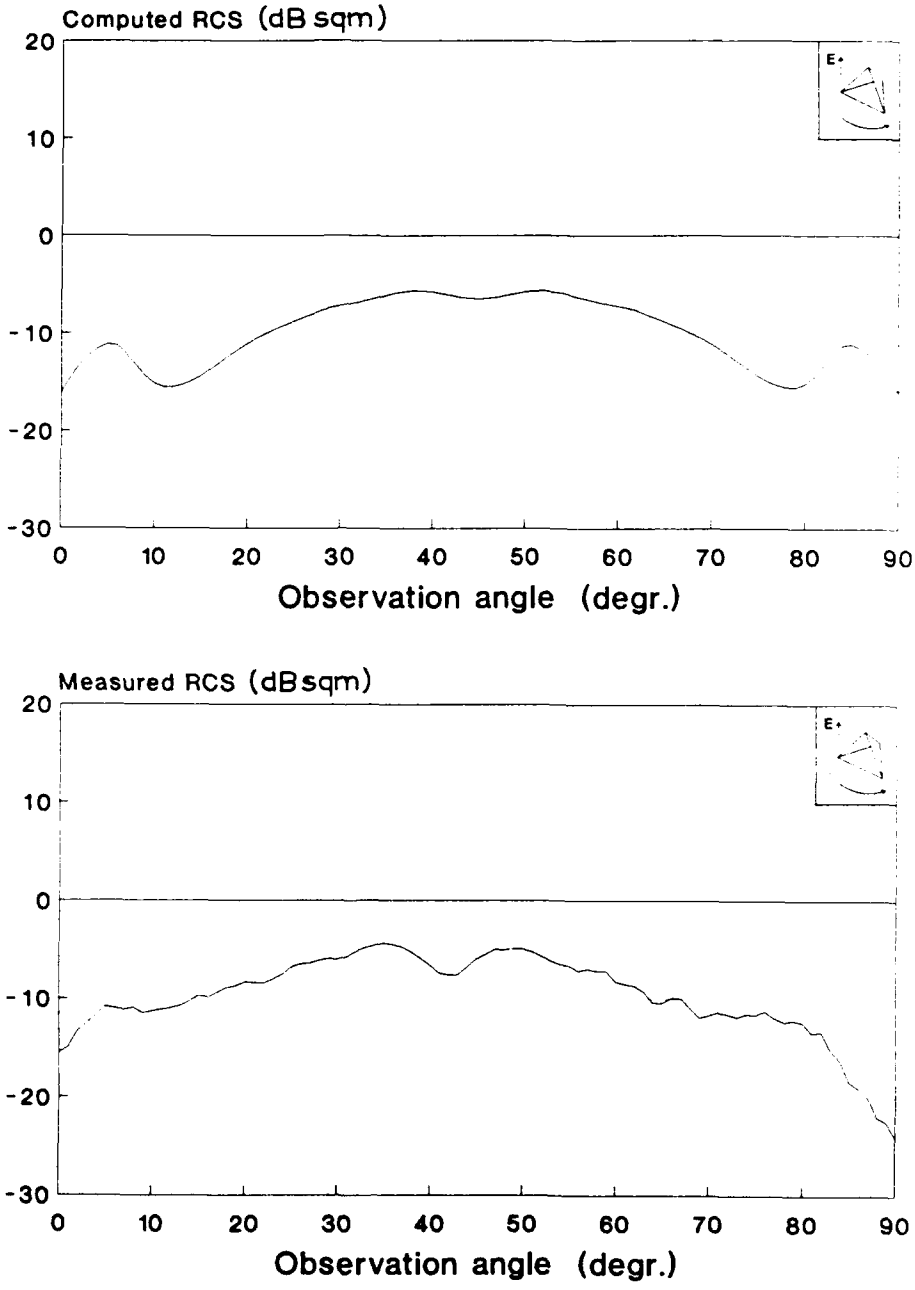

Fig. 11: Computed and measured RCS of the corner reflector at 16 GHz and vertical polarization.

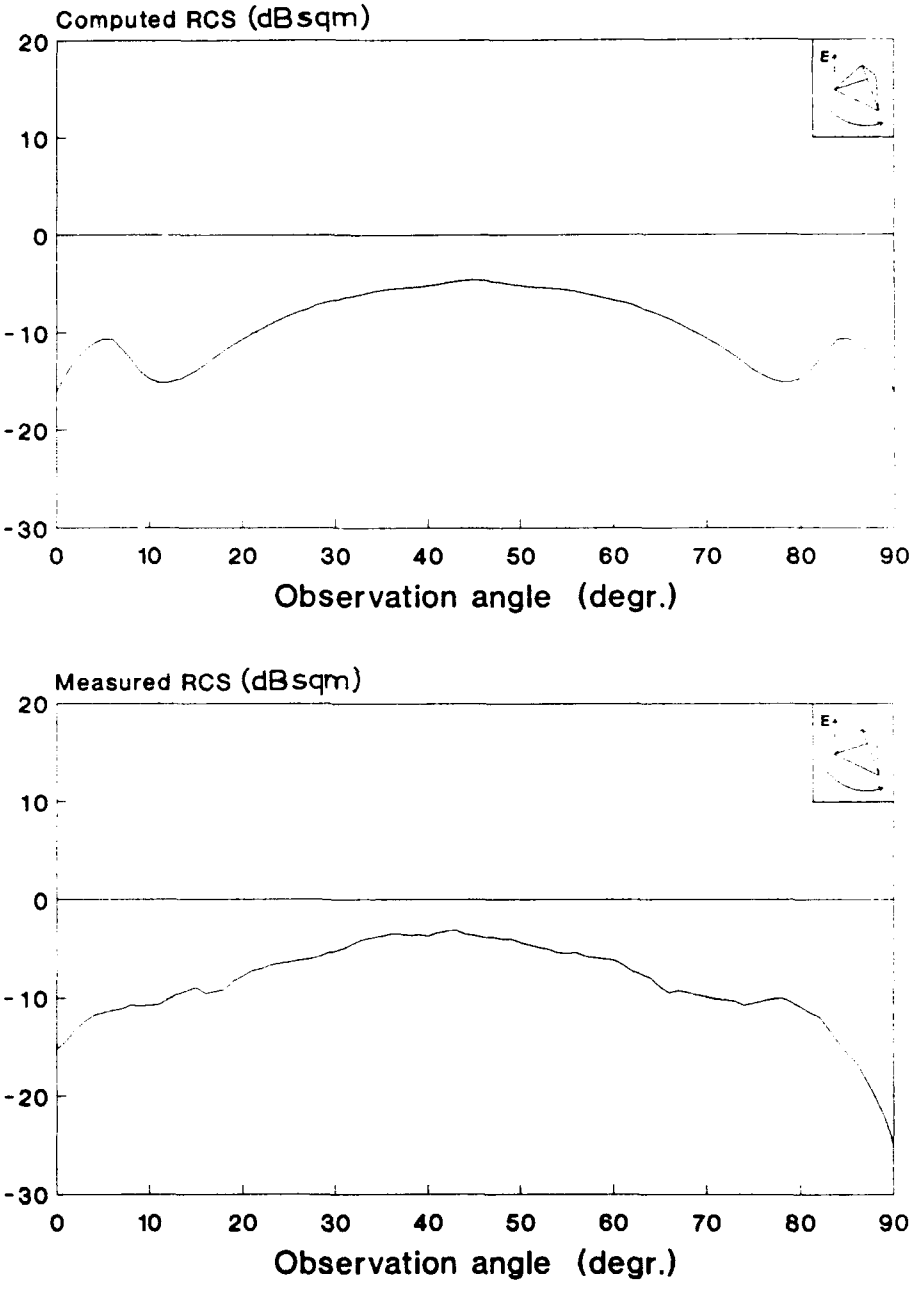

Fig. 12: Computed and measured RCS of the corner reflector at 17 GHz and vertical polarization.

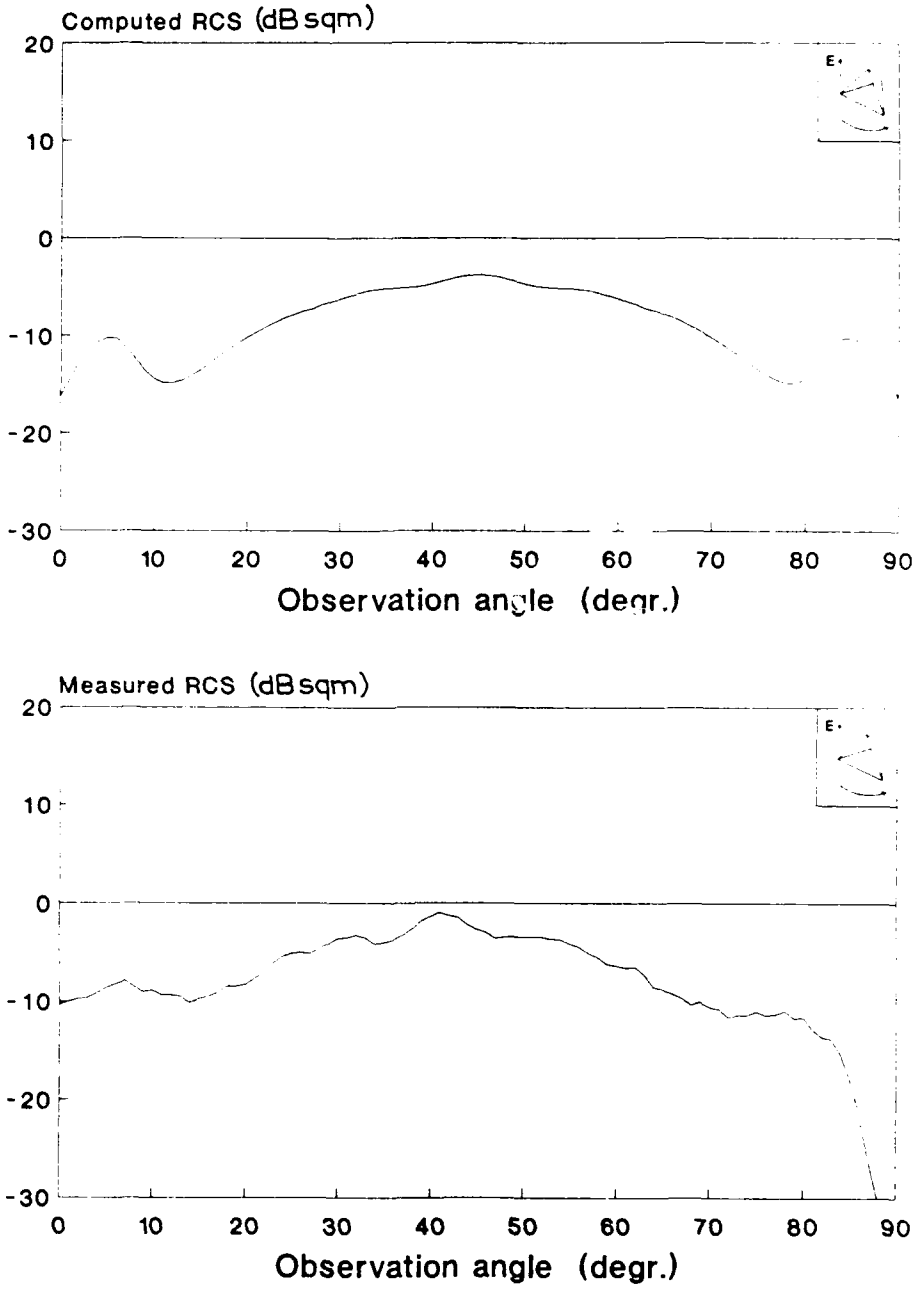

Fig. 13: Computed and measured RCS of the corner reflector at 18 GHz and vertical polarization.

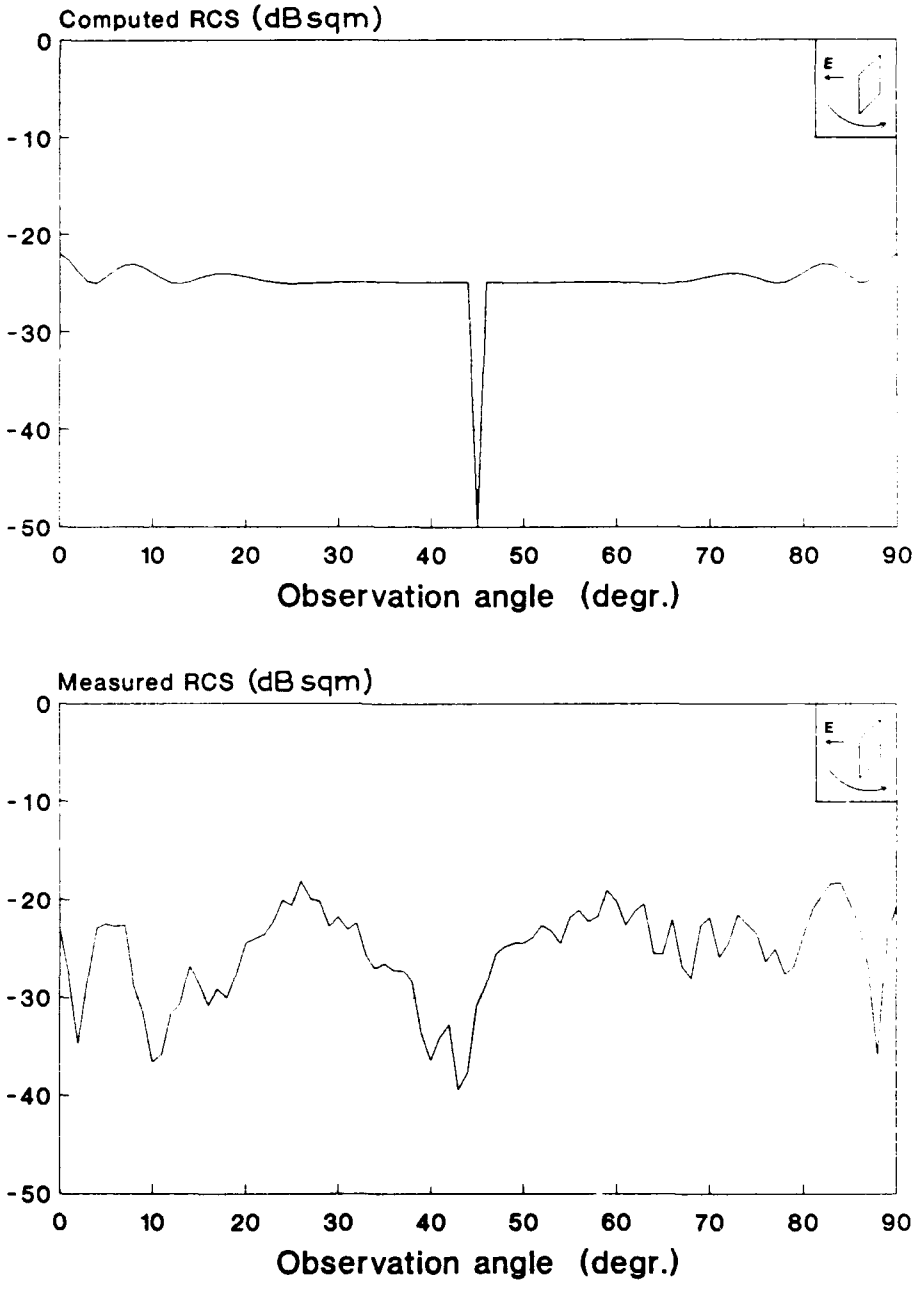

Fig. 14: Computed and measured RCS of the plate at 16 GHz and horizontal polarization.

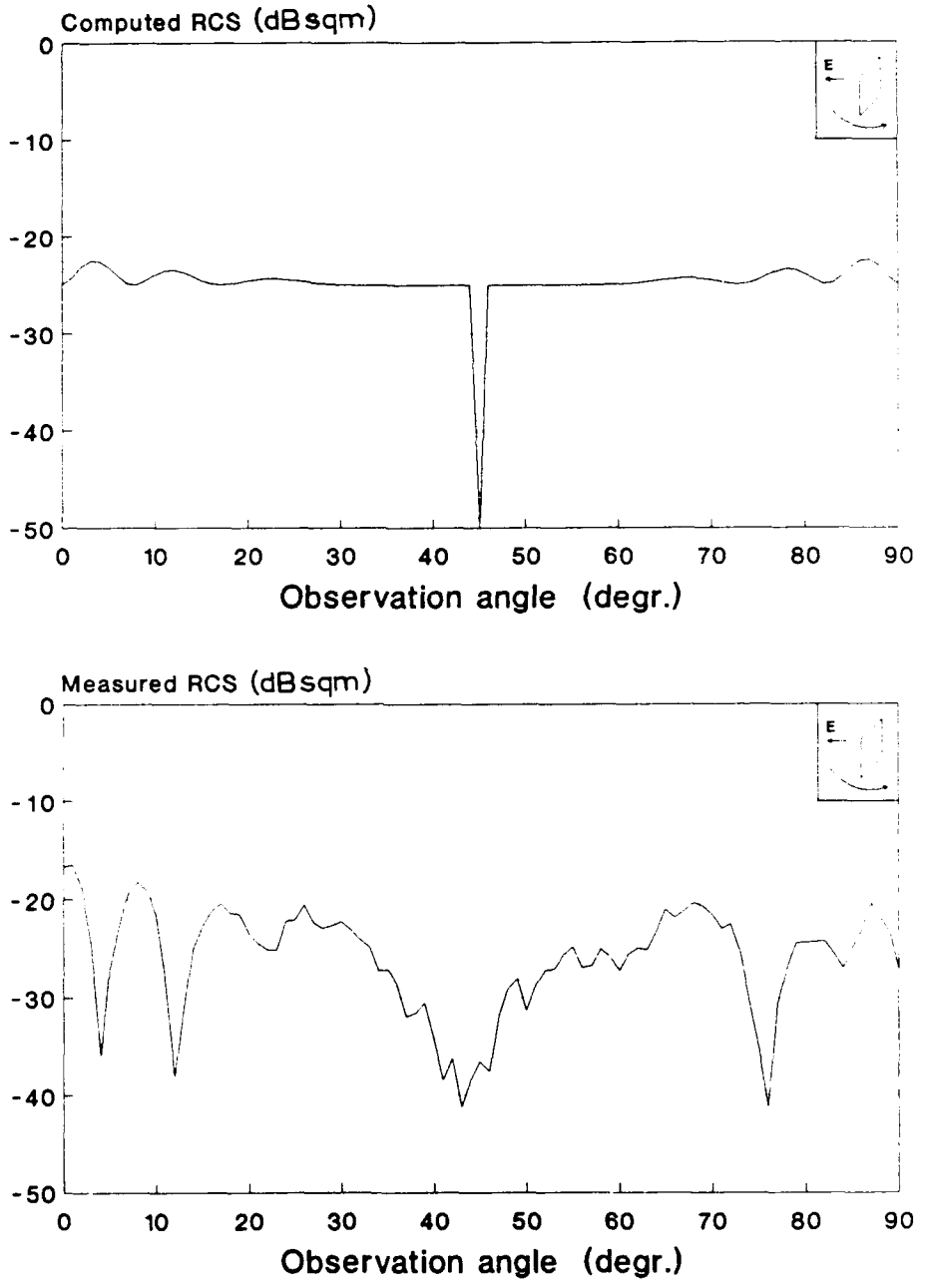

Fig. 15: Computed and measured RCS of the plate at 17 GHz and horizontal polarization.

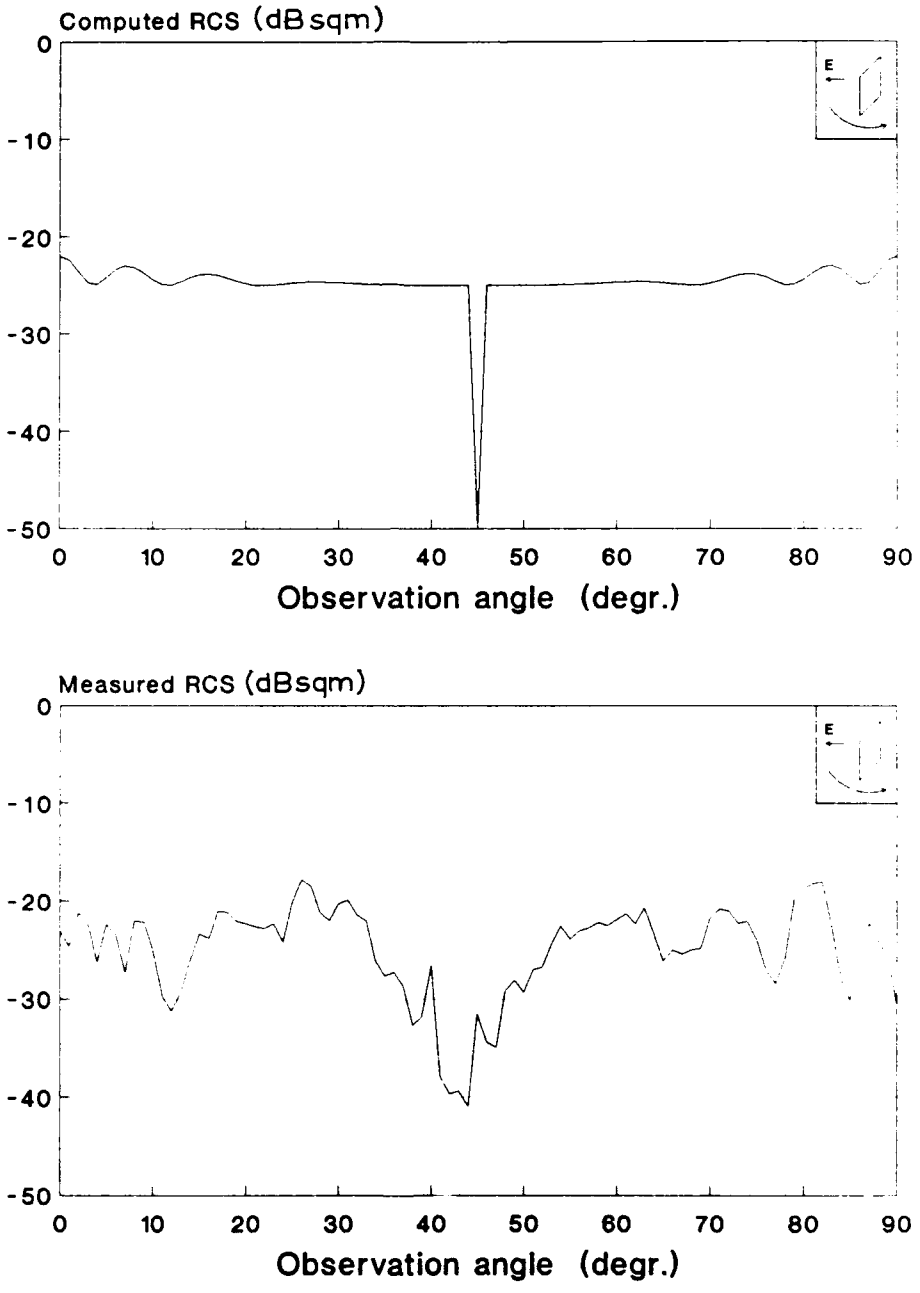

Fig. 16: Computed and measured RCS of the plate at 18 GHz and horizontal polarization.

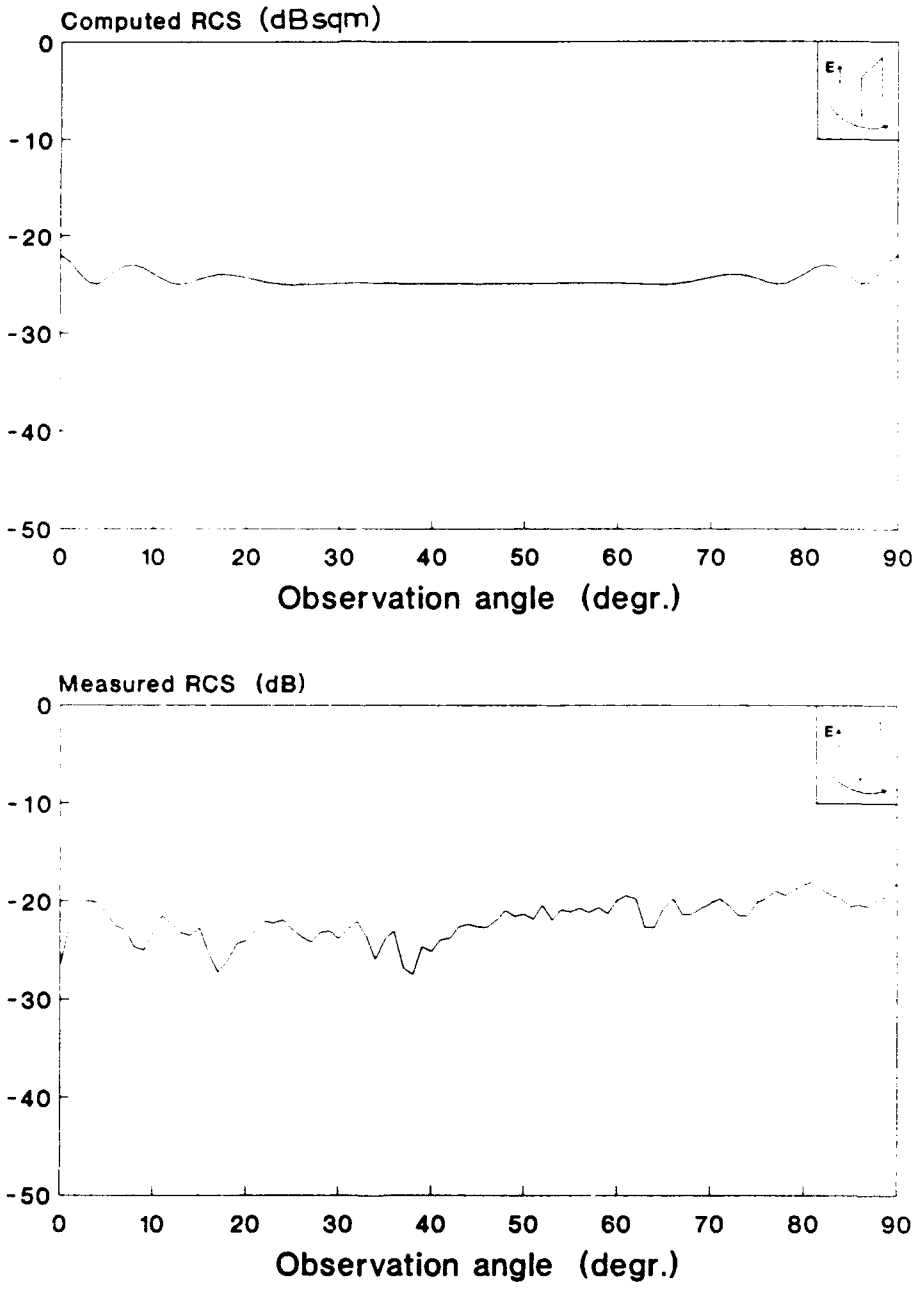

Fig. 17: Computed and measured RCS of the plate at 16 GHz and vertical polarization.

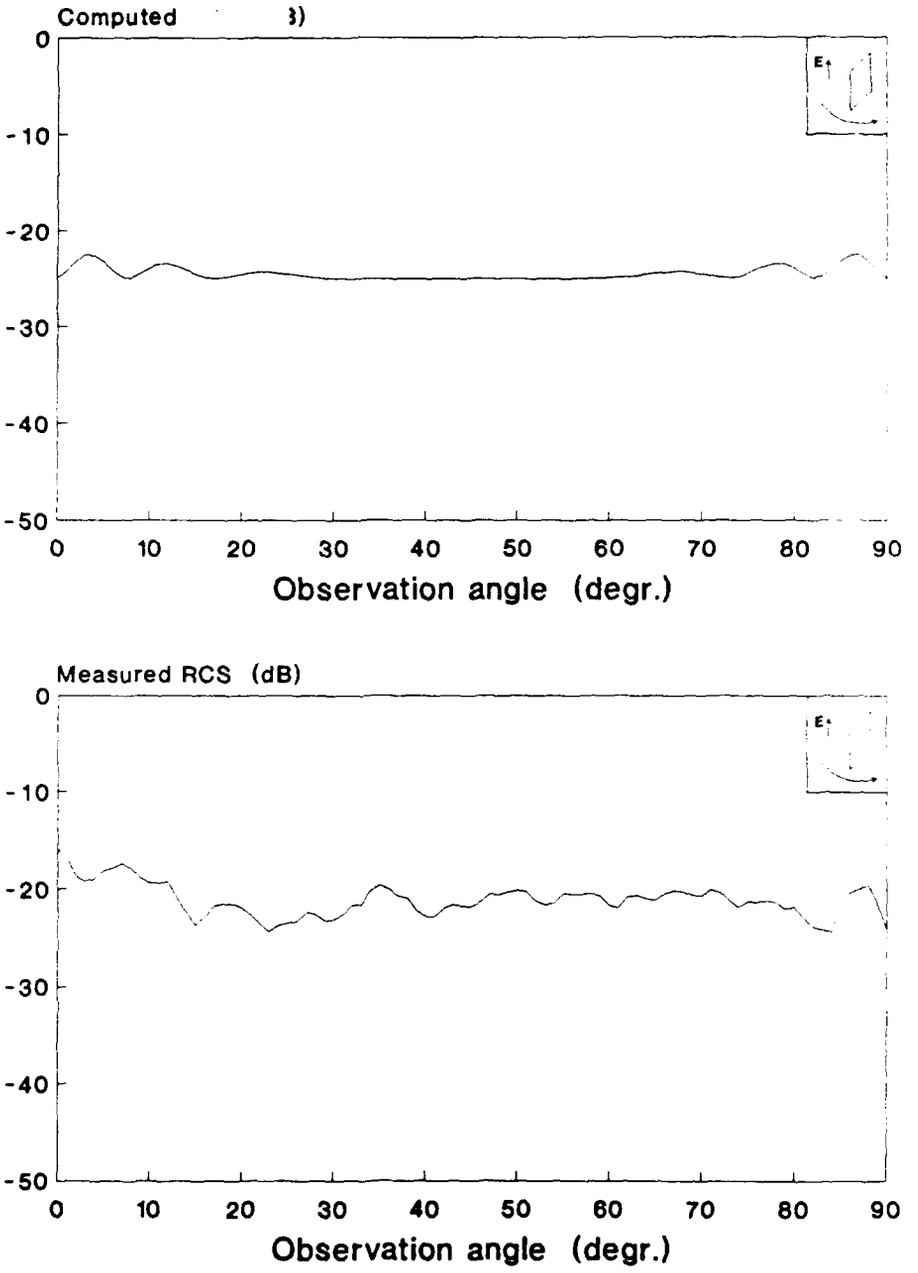

Fig. 18: Computed and measured RCS of the plate at 17 GHz and vertical polarization.

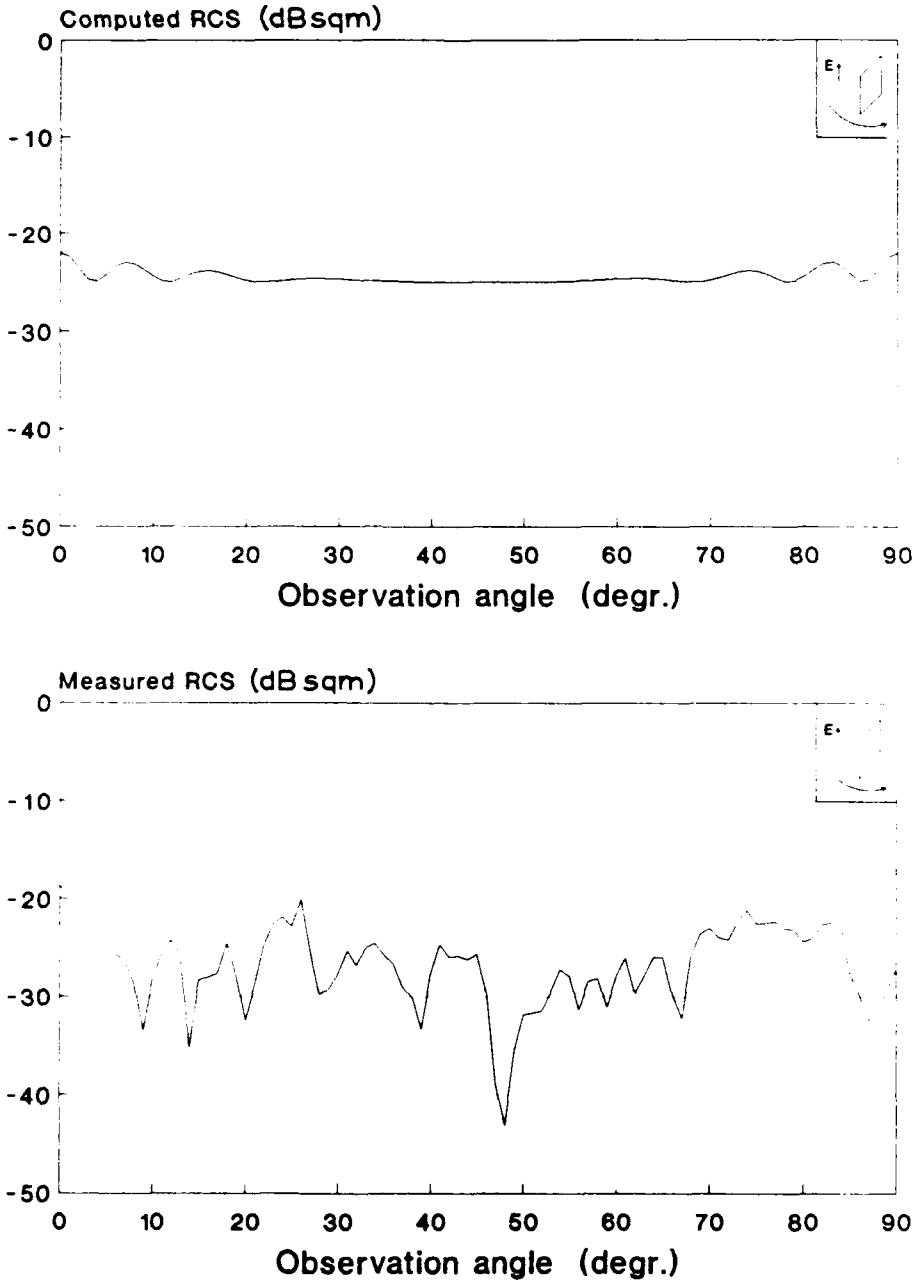

Fig. 19: Computed and measured RCS of the plate at 18 GHz and vertical polarization.

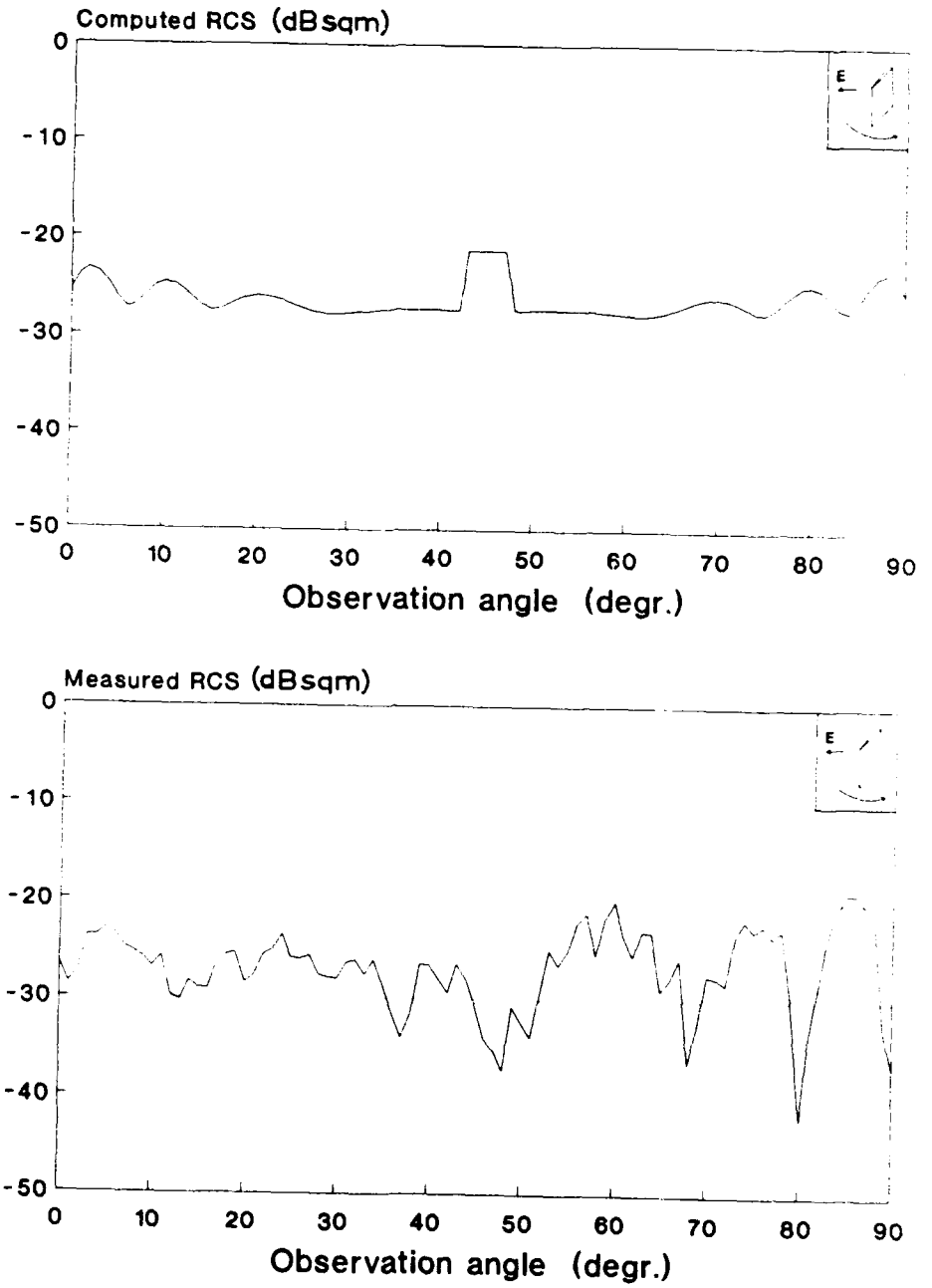

Fig. 20: Computed and measured RCS of Wedge05 at 16 GHz and horizontal polarization.

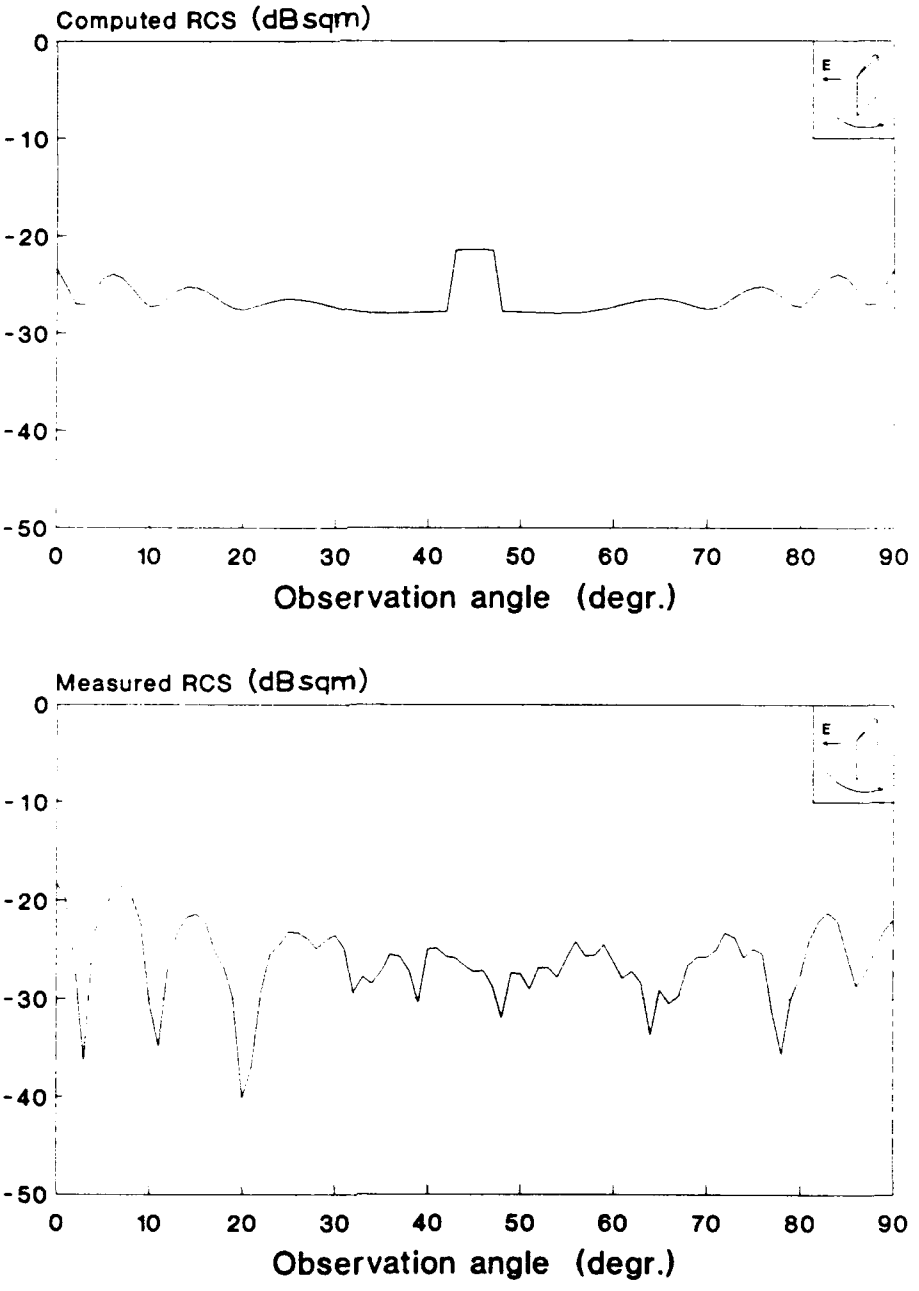

Fig. 21: Computed and measured RCS of Wedge05 at 17 GHz and horizontal polarization.

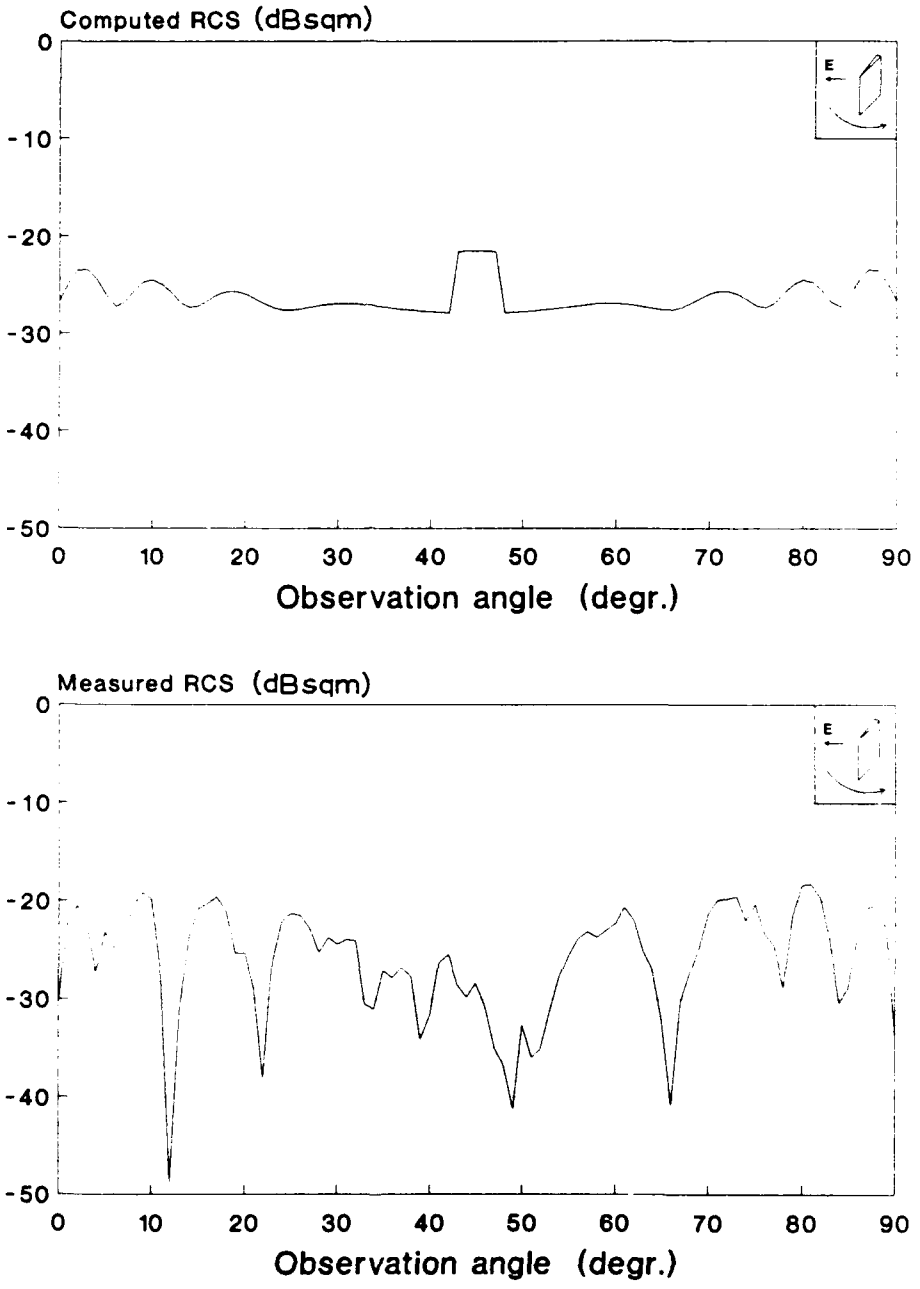

Fig. 22: Computed and measured RCS of Wedge05 at 18 GHz and horizontal polarization.

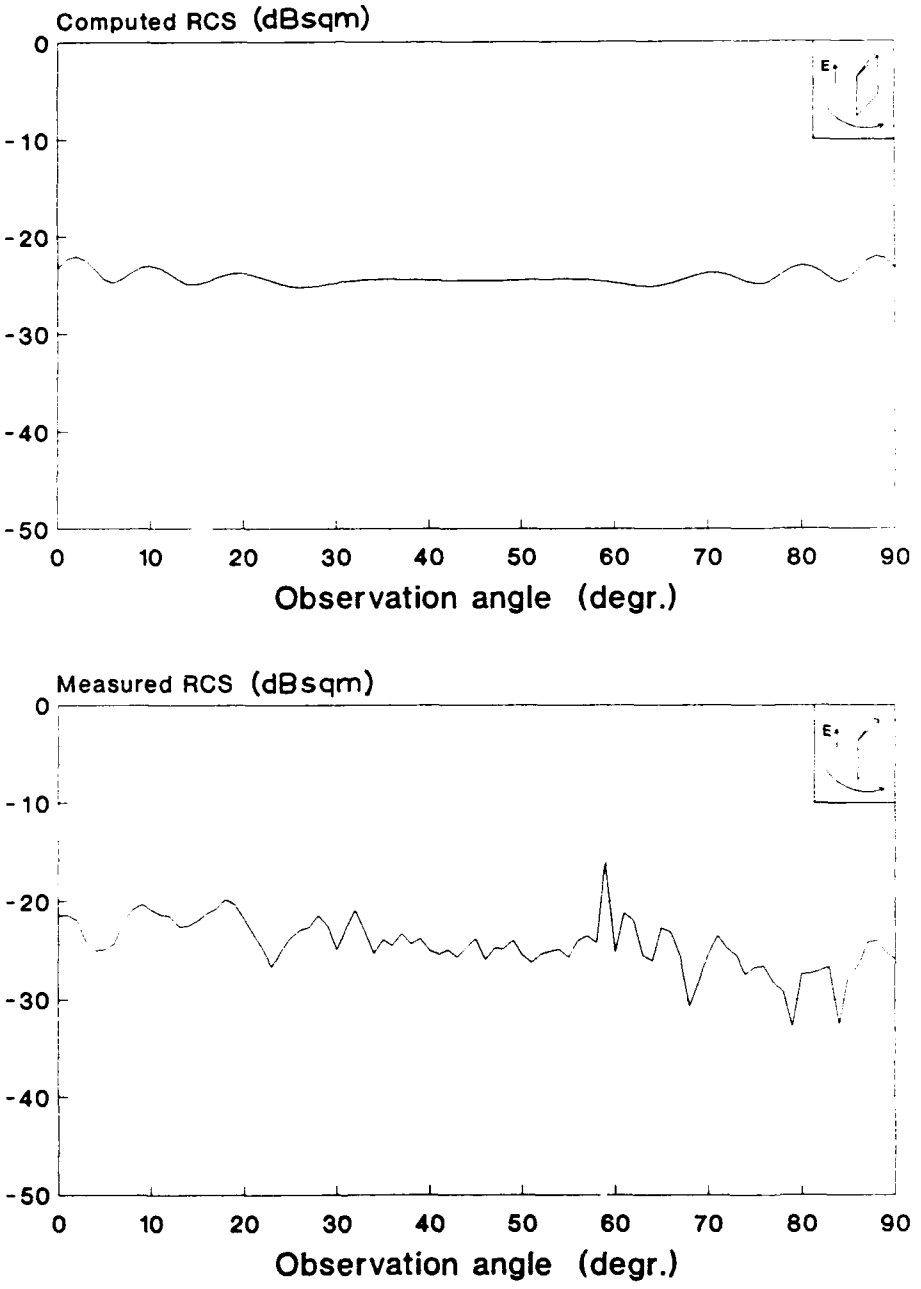

Fig. 23: Computed and measured RCS of Wedge05 at 16 GHz and vertical polarization.

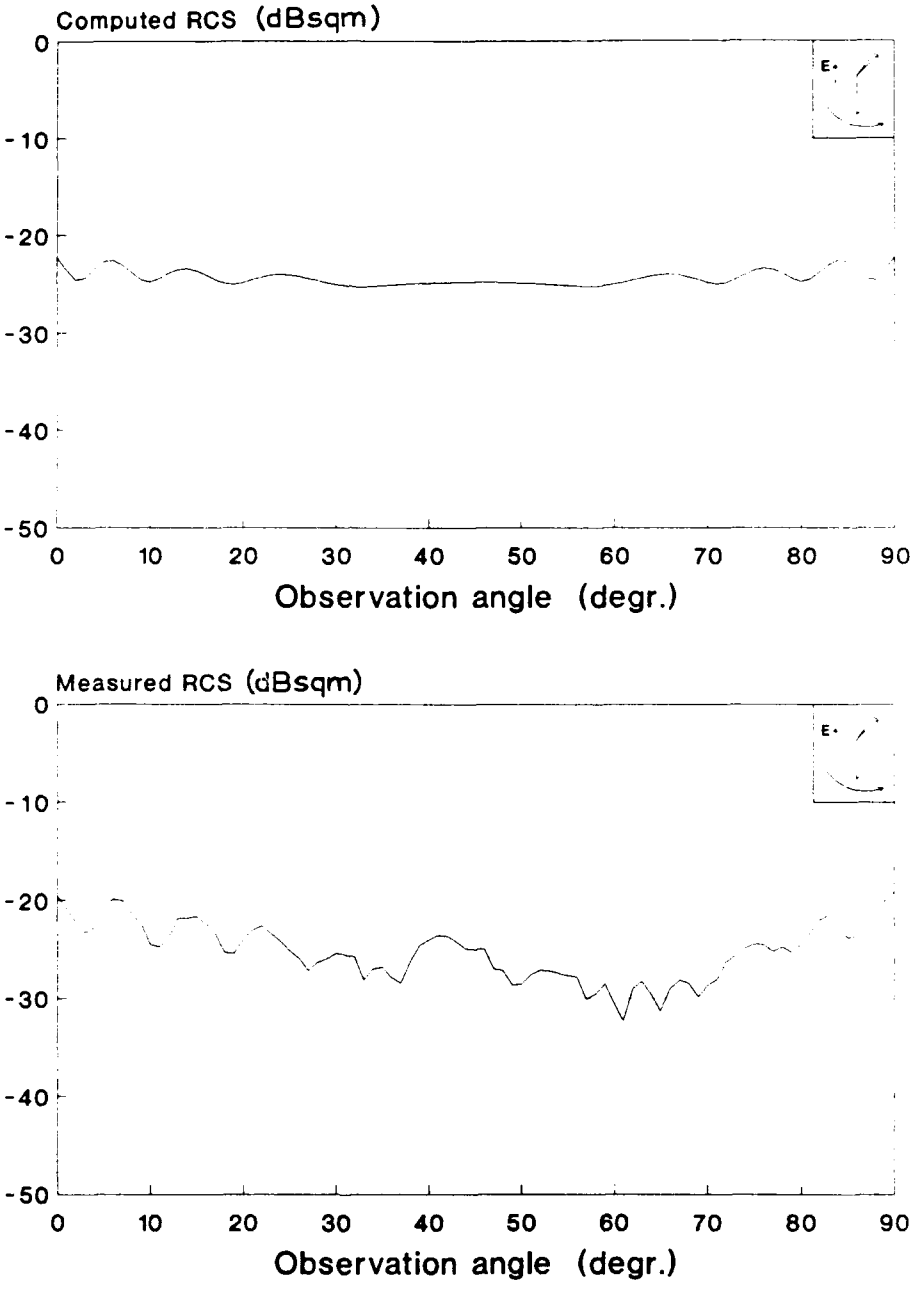

Fig. 24: Computed and measured RCS of Wedge05 at 17 GHz and vertical polarization.

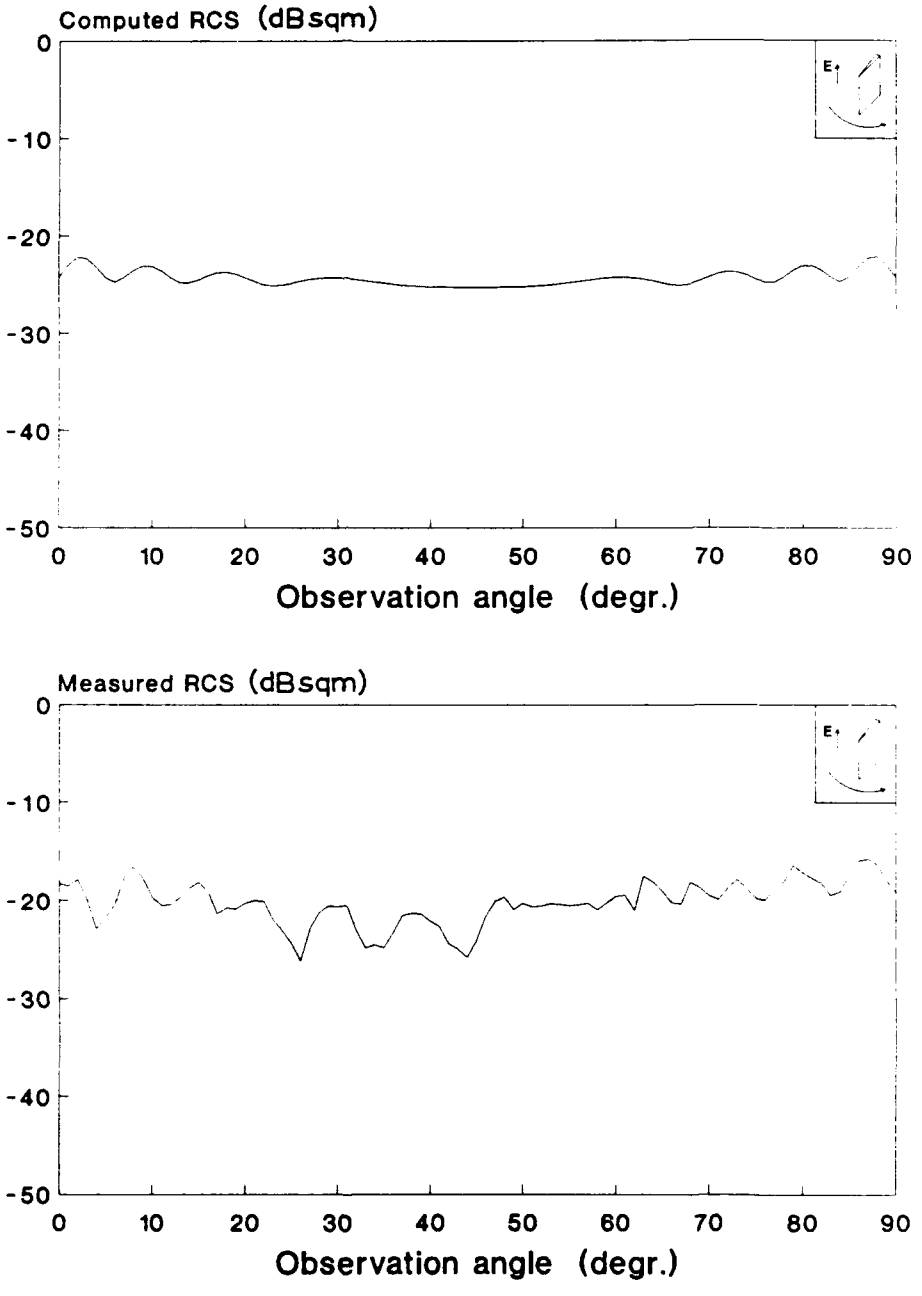

Fig. 25: Computed and measured RCS of Wedge05 at 18 GHz and vertical polarization.

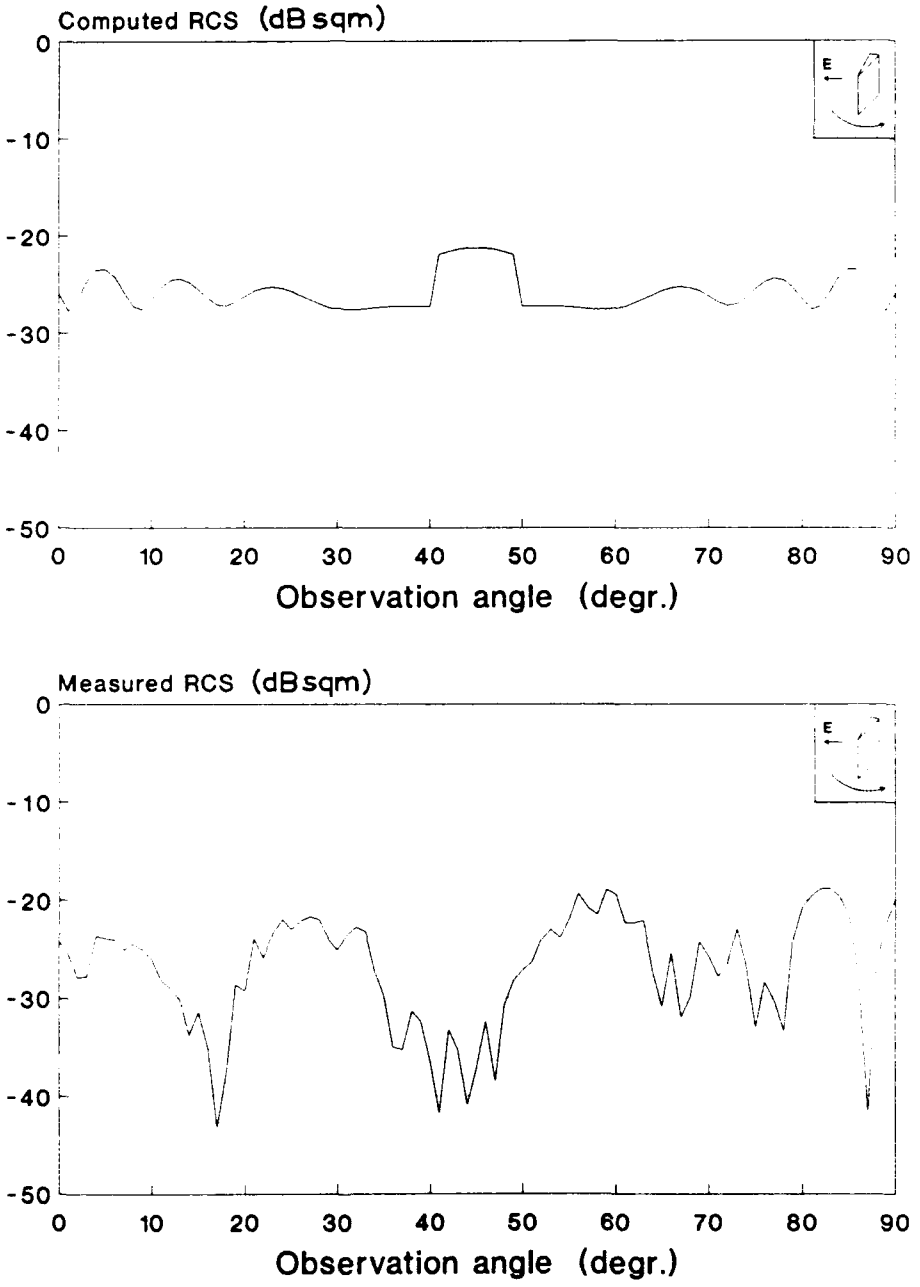

Fig. 26: Computed and measured RCS of Wedge10 at 16 GHz and horizontal polarization.

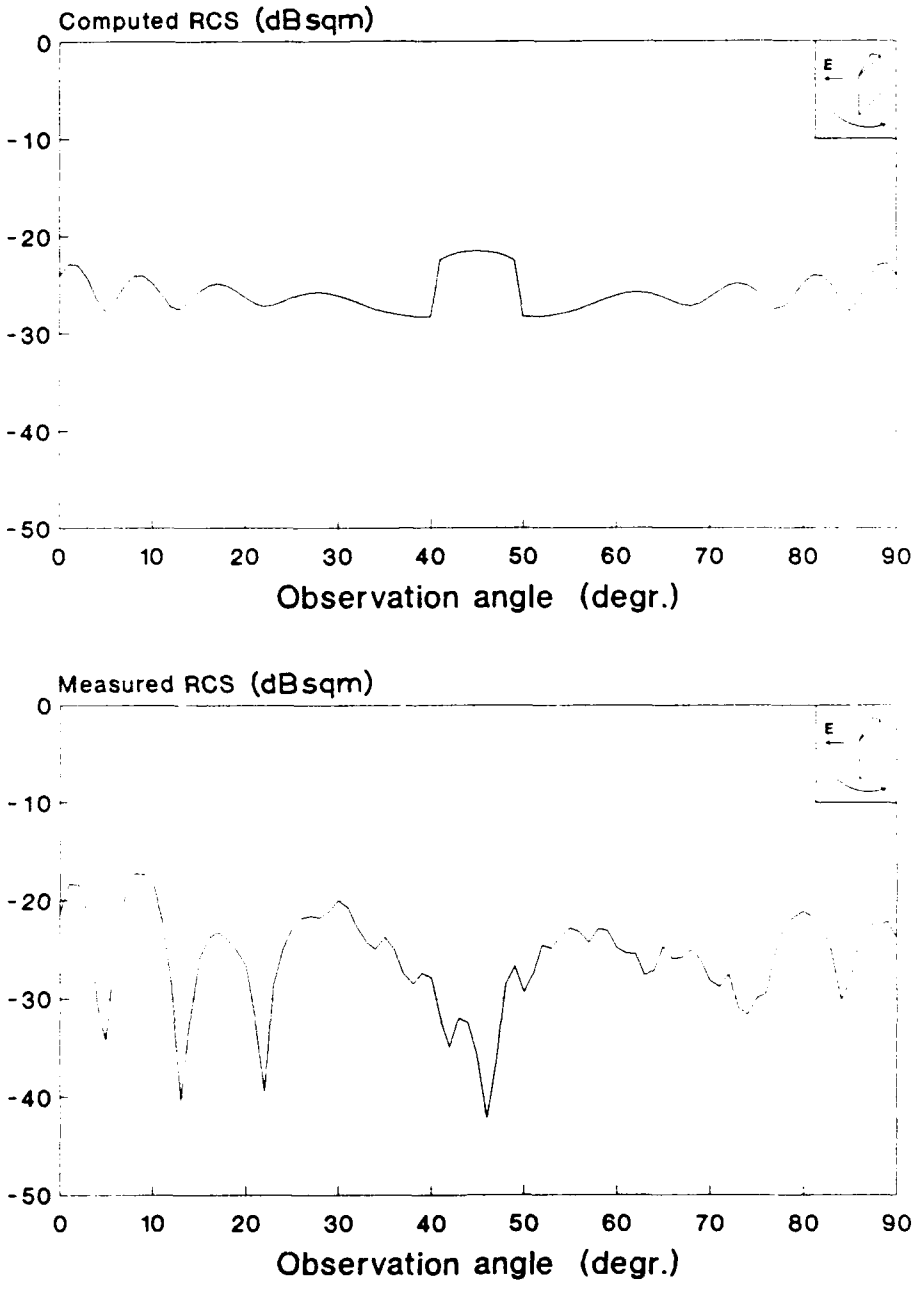

Fig. 27: Computed and measured RCS of Wedge10 at 17 GHz and horizontal polarization.

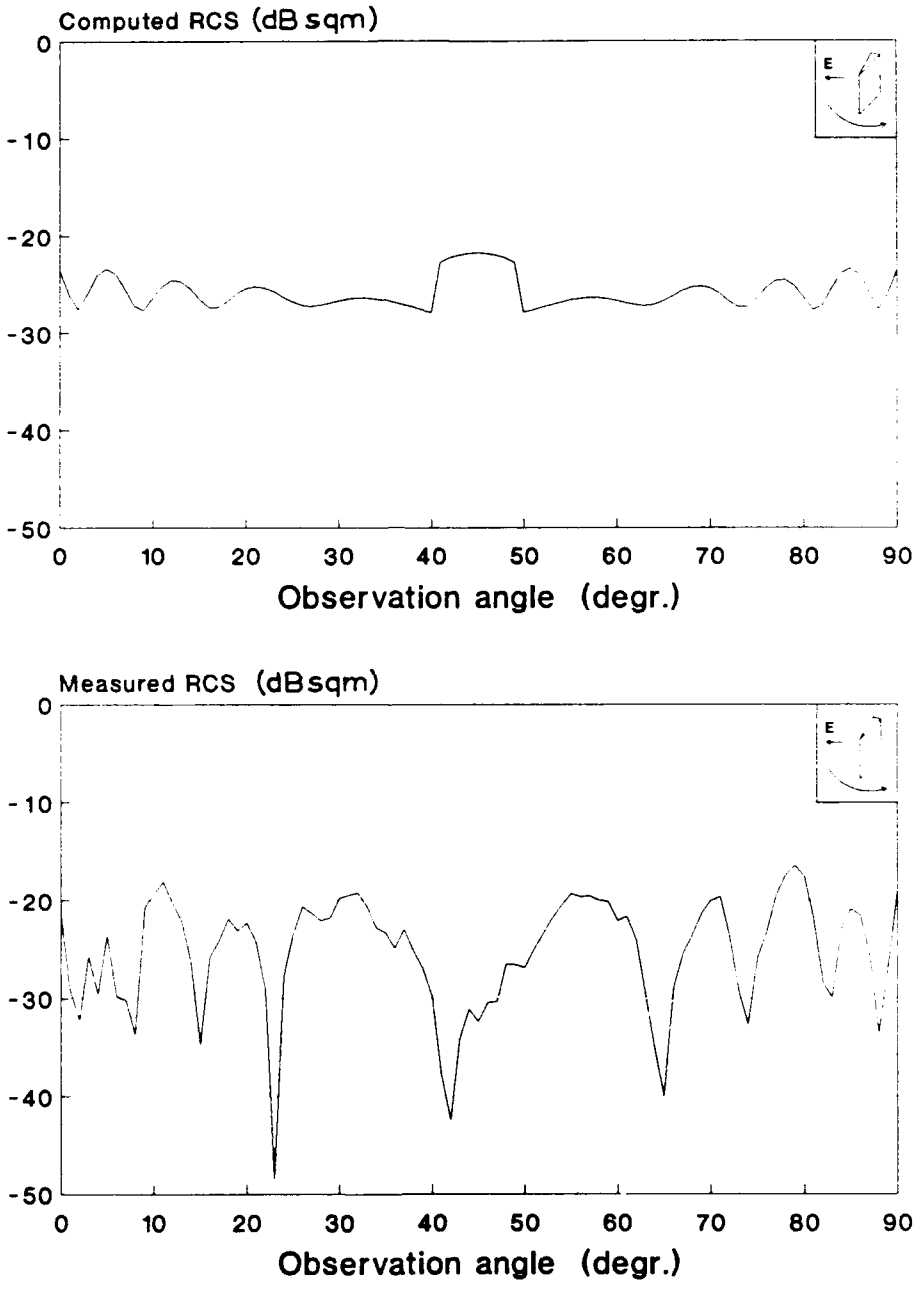

Fig. 28: Computed and measured RCS of Wedge10 at 18 GHz and horizontal polarization.

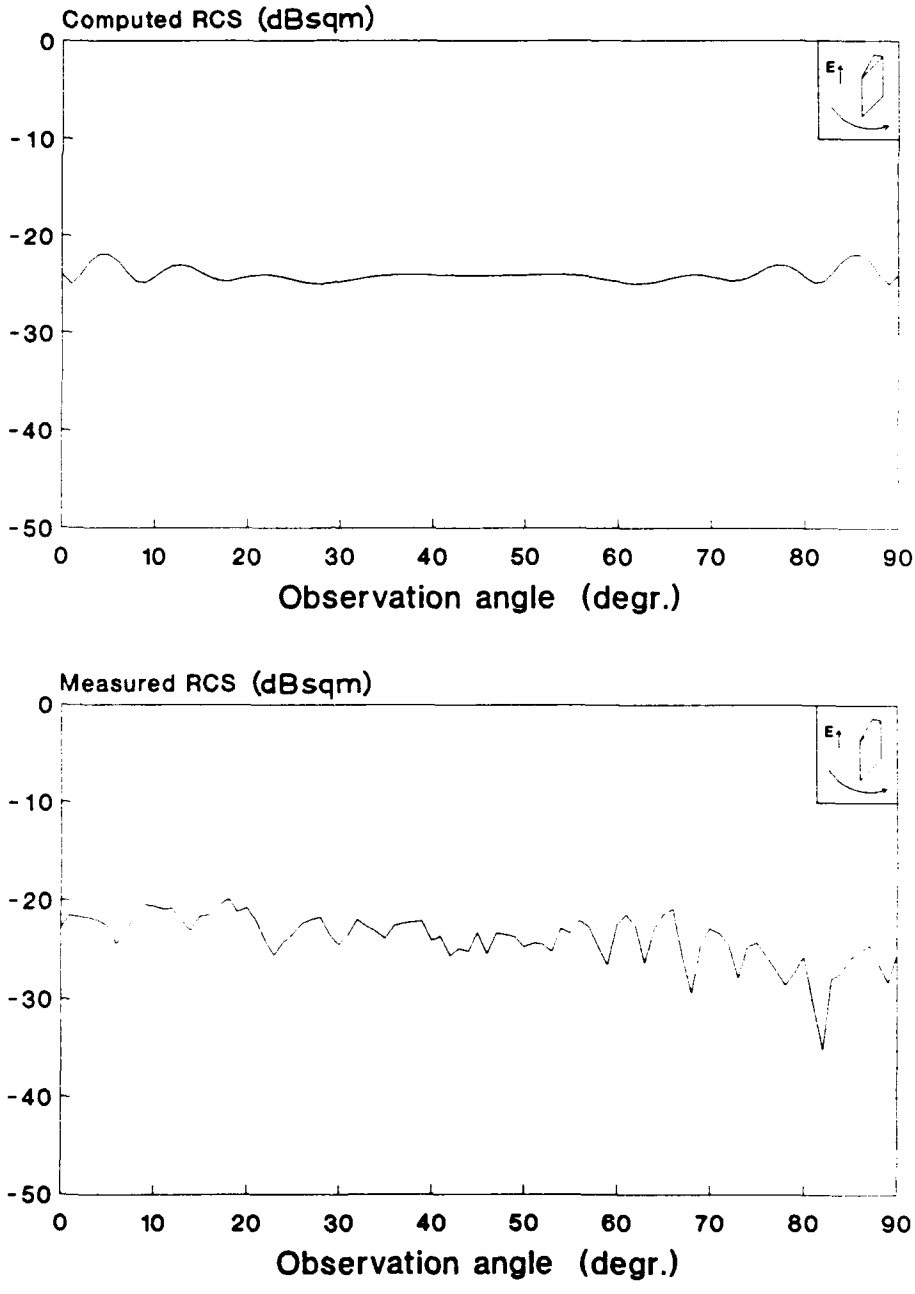

Fig. 29: Computed and measured RCS of Wedge10 at 16 GHz and vertical polarization.

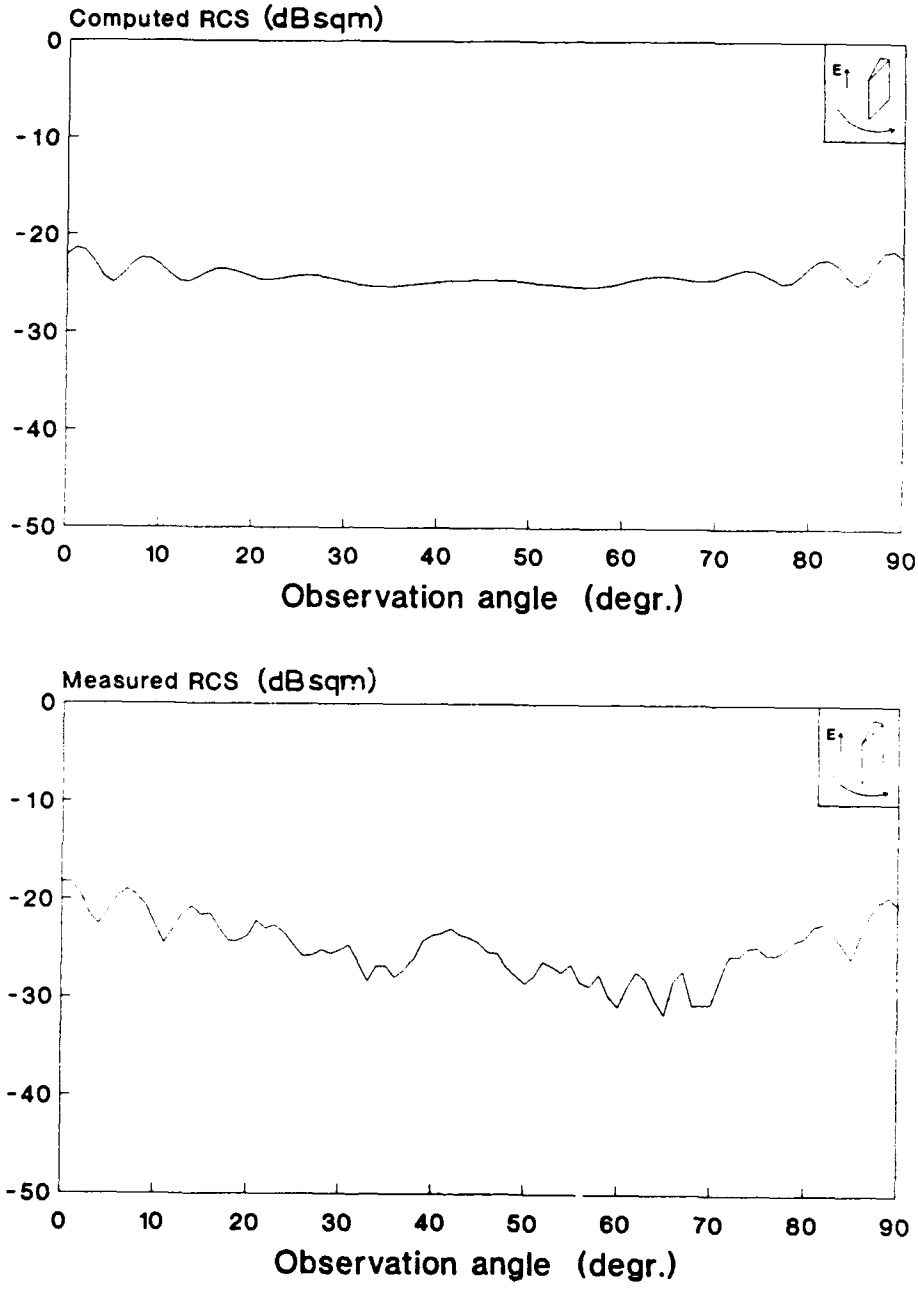

Fig. 30: Computed and measured RCS of Wedge10 at 17 GHz and vertical polarization.

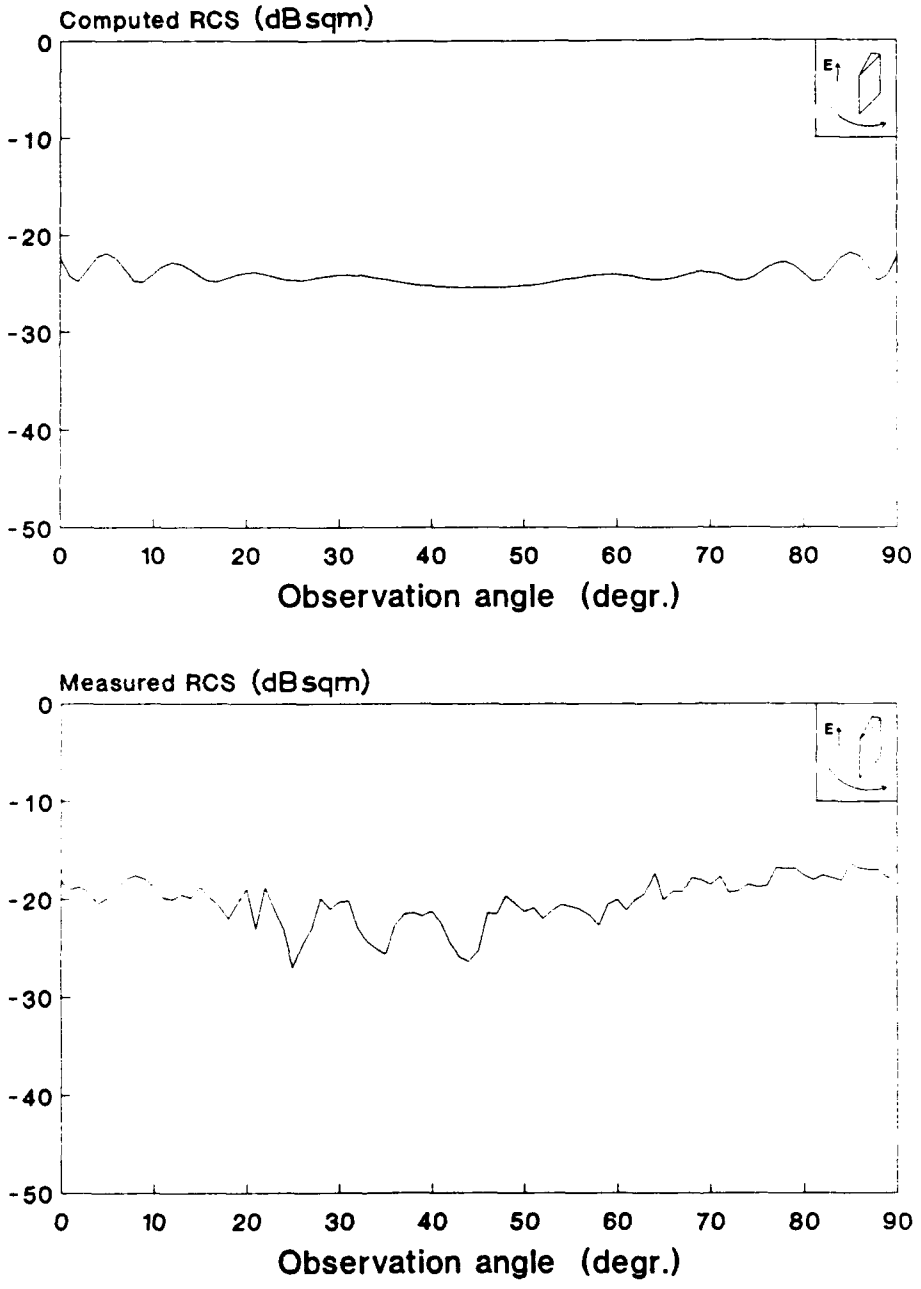

Fig. 31: Computed and measured RCS of Wedge10 at 18 GHz and vertical polarization.

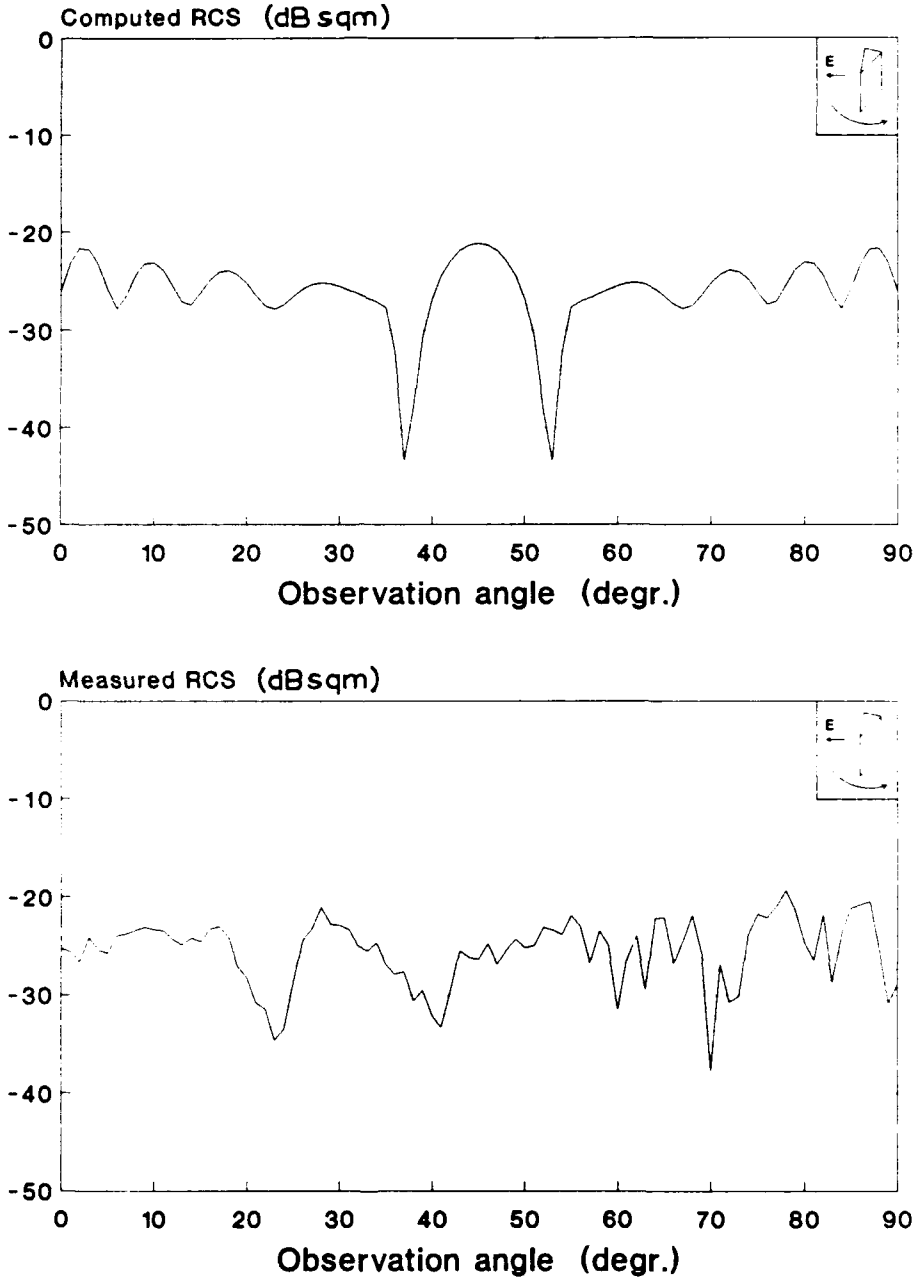

Fig. 32: Computed and measured RCS of Wedge20 at 16 GHz and horizontal polarization.

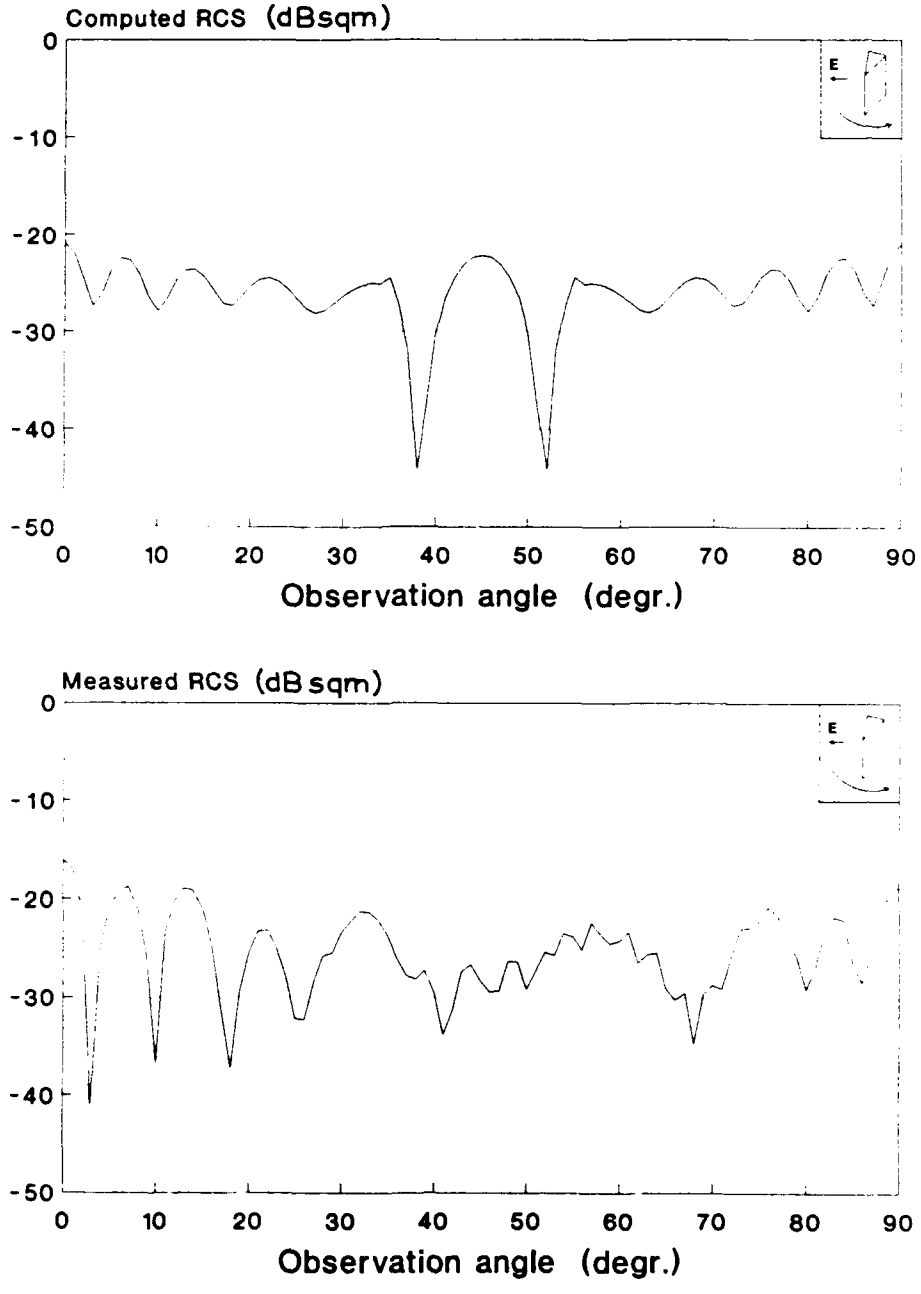

Fig. 33: Computed and measured RCS of Wedge20 at 17 GHz and horizontal polarization.

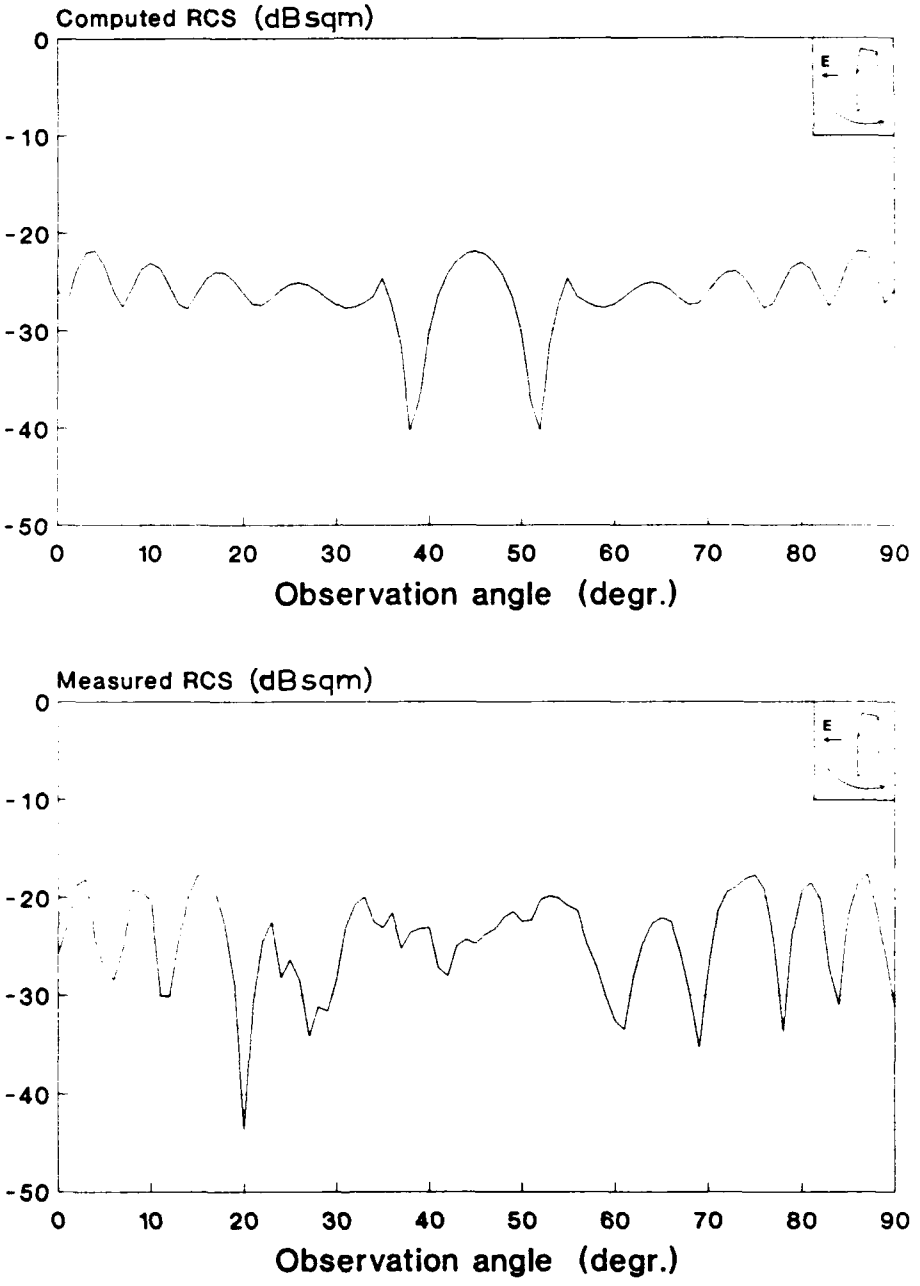

Fig. 34: Computed and measured RCS of Wedge20 at 18 GHz and horizontal polarization.

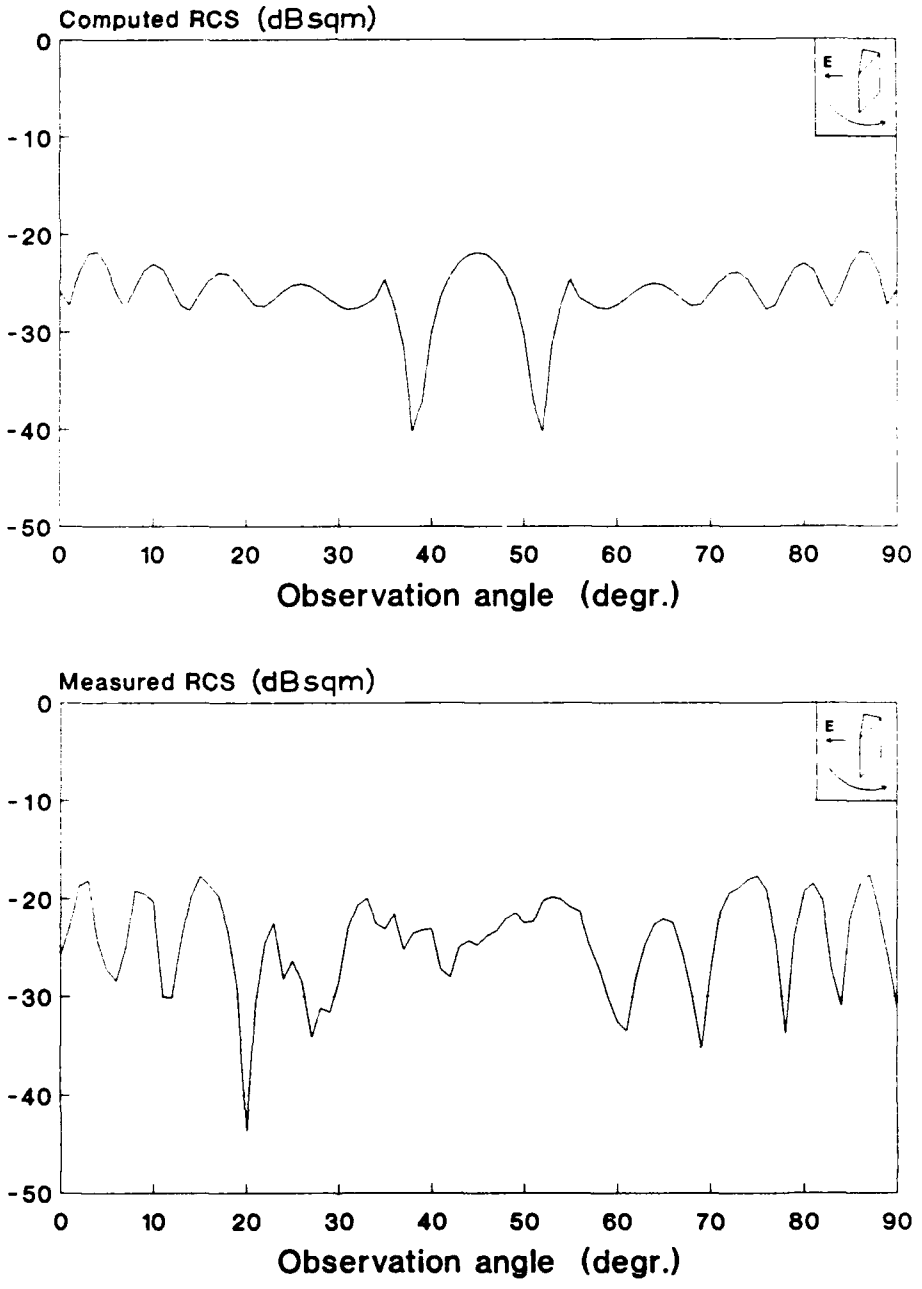

Fig. 34: Computed and measured RCS of Wedge20 at 18 GHz and horizontal polarization.

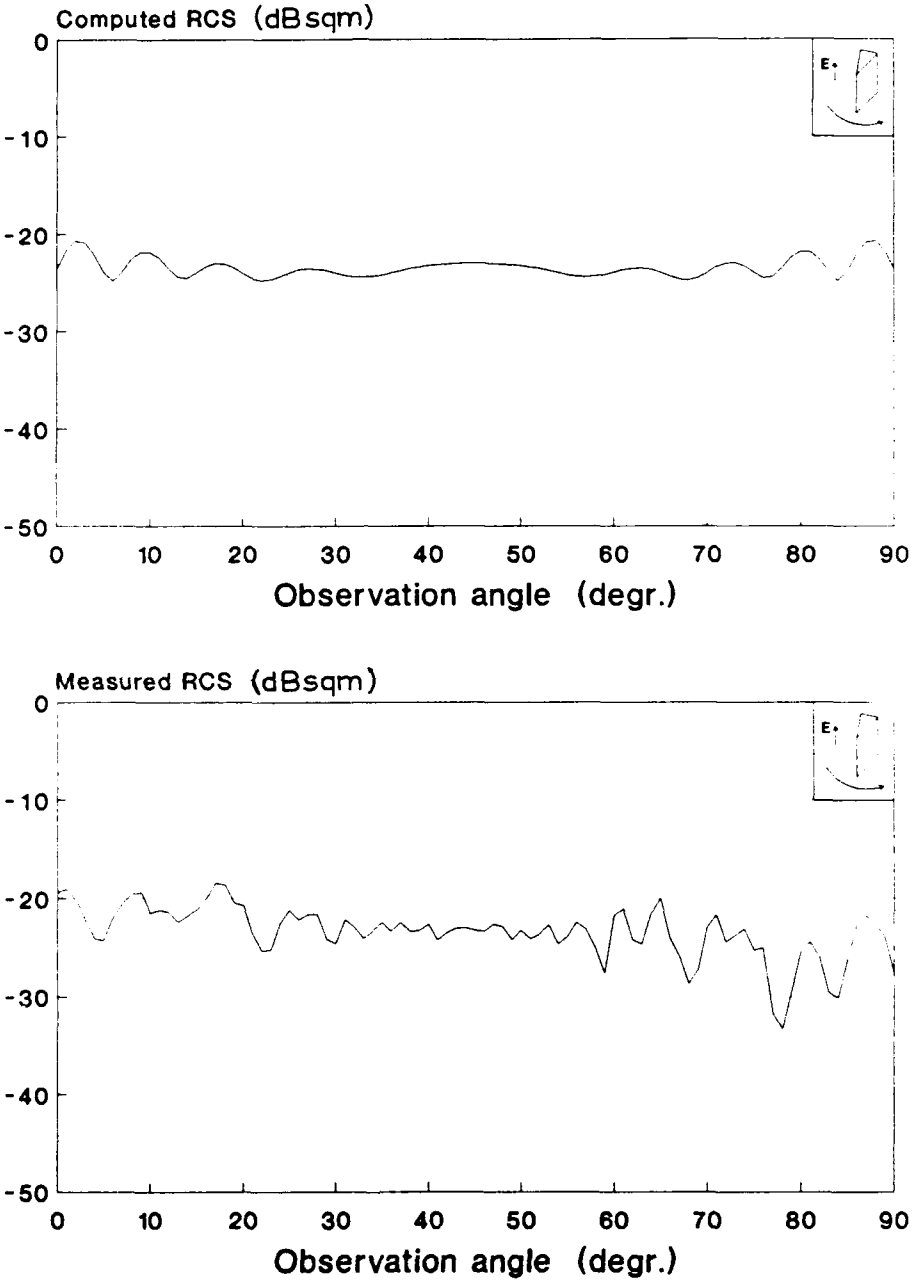

Fig. 35: Computed and measured RCS of Wedge20 at 16 GHz and vertical polarization.

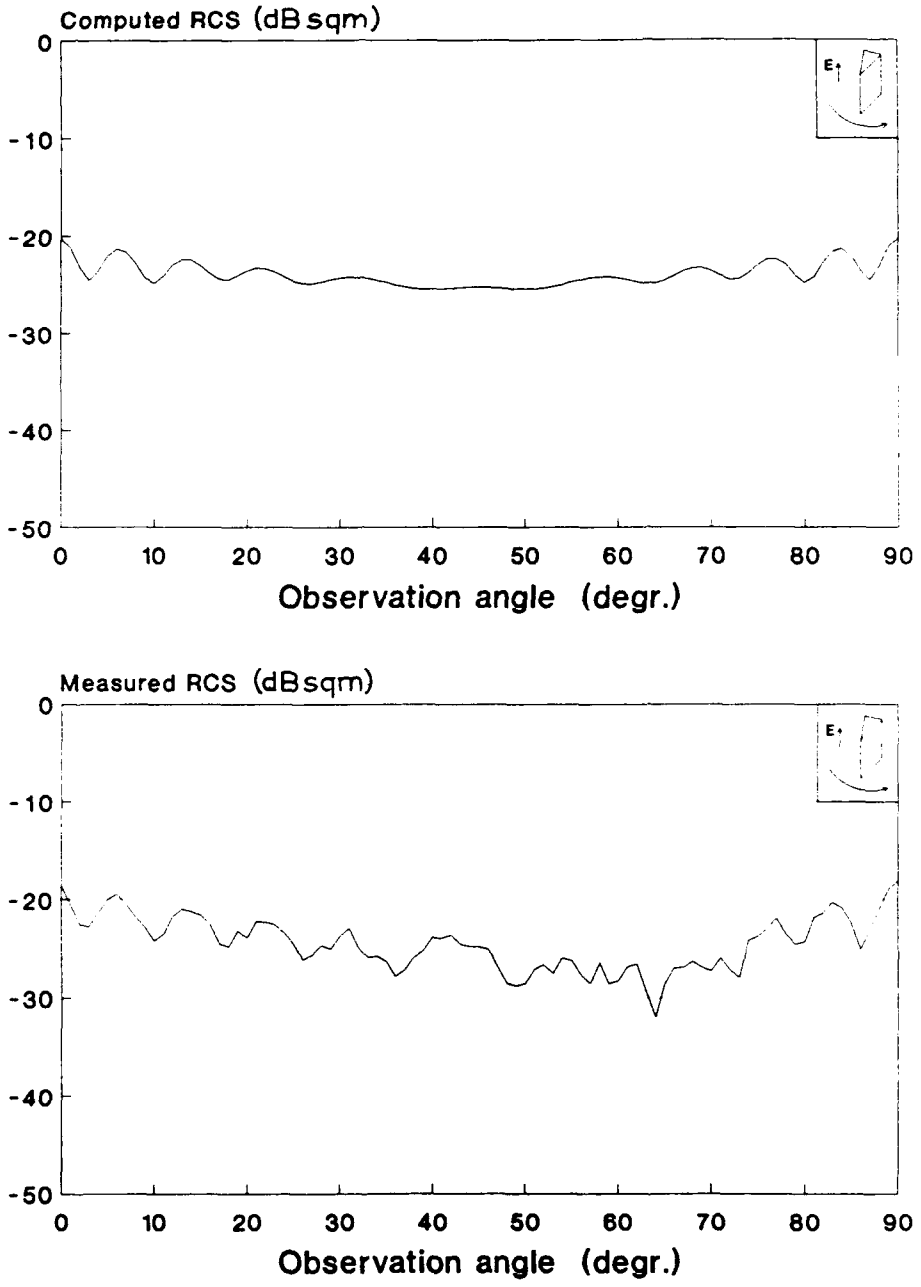

Fig. 36: Computed and measured RCS of Wedge20 at 17 GHz and vertical polarization.

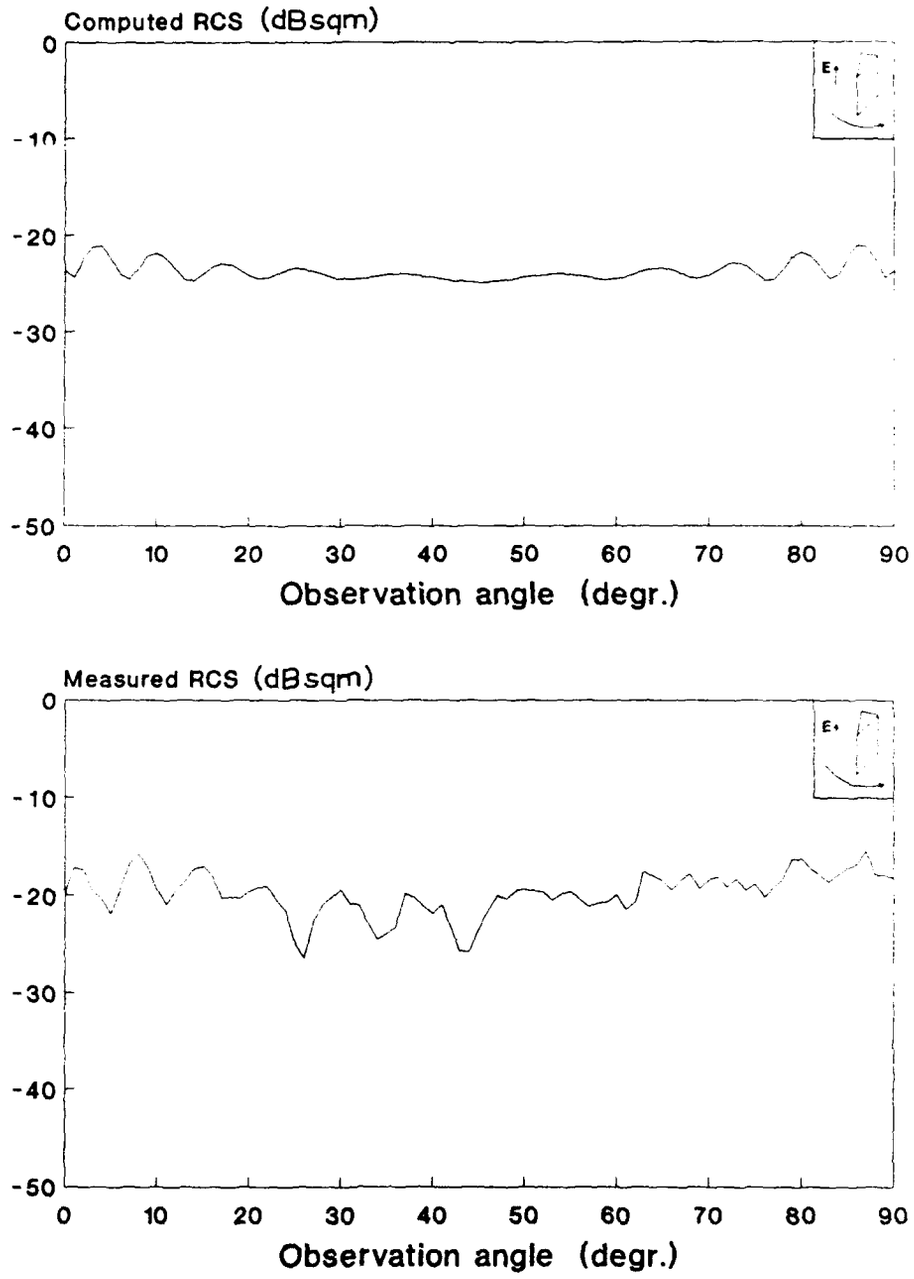

Fig. 37: Computed and measured RCS of Wedge20 at 18 GHz and vertical polarization.

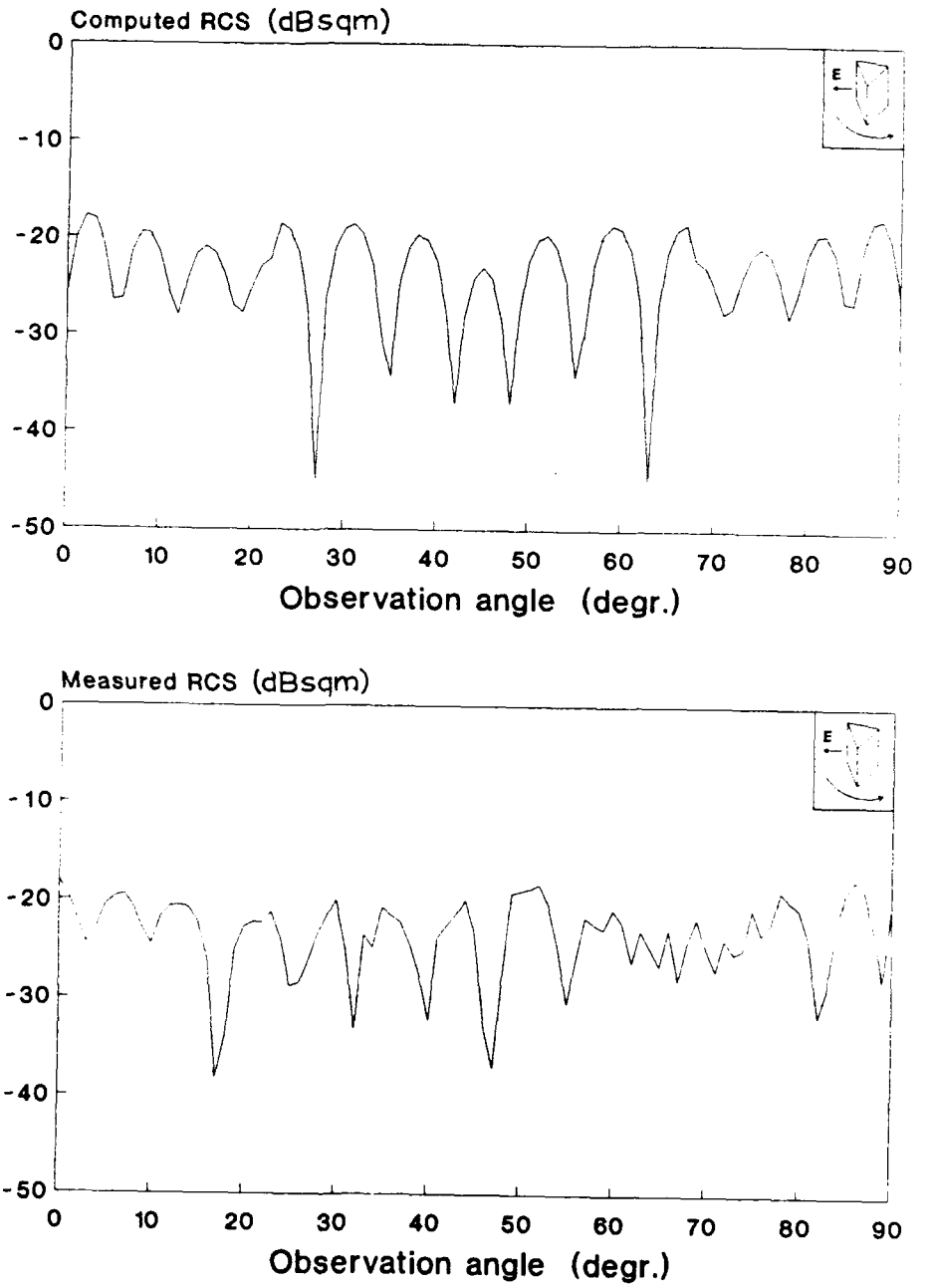

Fig. 38: Computed and measured RCS of Wedge45 at 16 GHz and horizontal polarization.

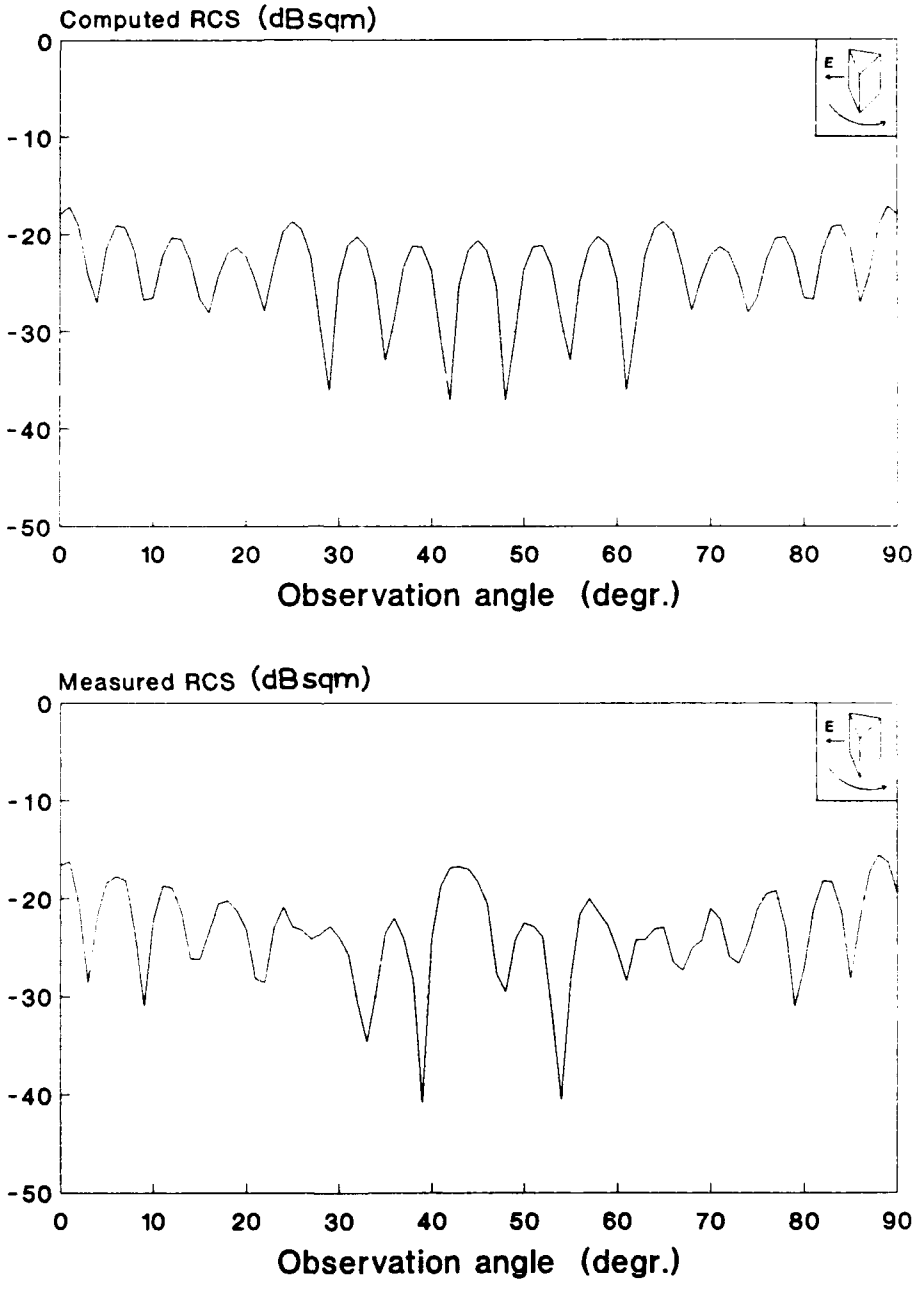

Fig. 39: Computed and measured RCS of Wedge45 at 17 GHz and horizontal polarization.

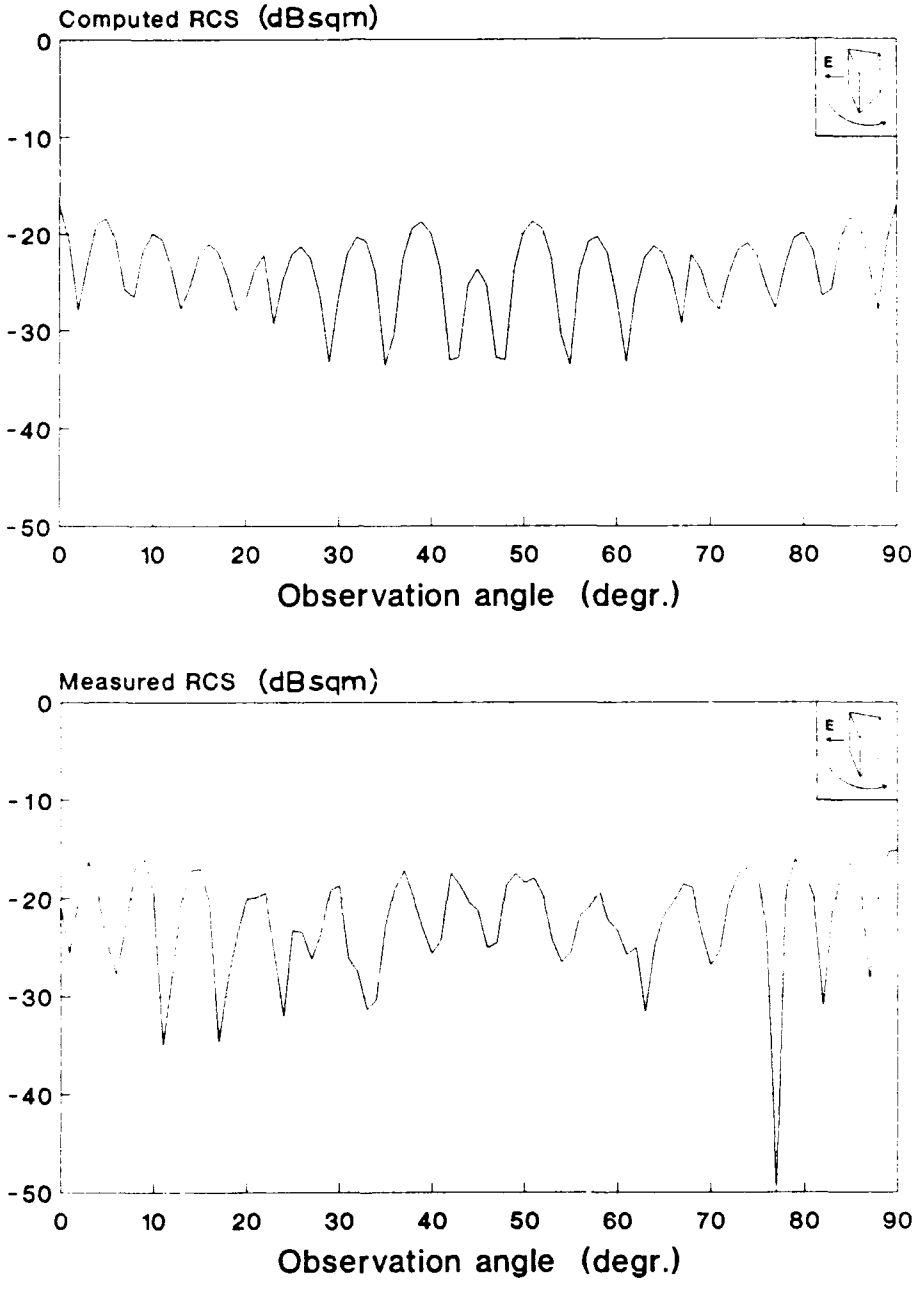

Fig. 40: Computed and measured RCS of Wedge45 at 18 GHz and horizontal polarization.

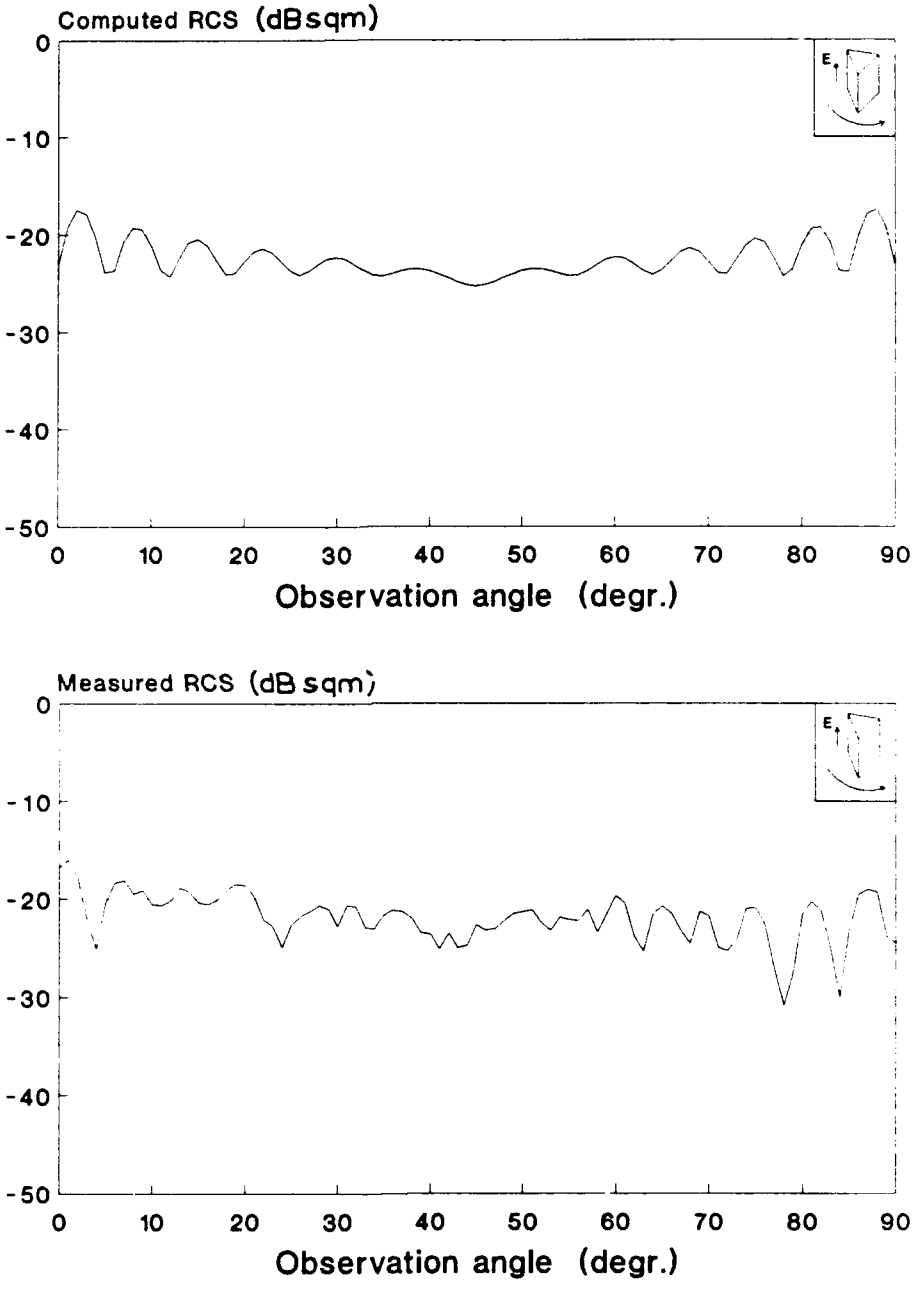

Fig. 41: Computed and measured RCS of Wedge45 at 16 GHz and vertical polarization.

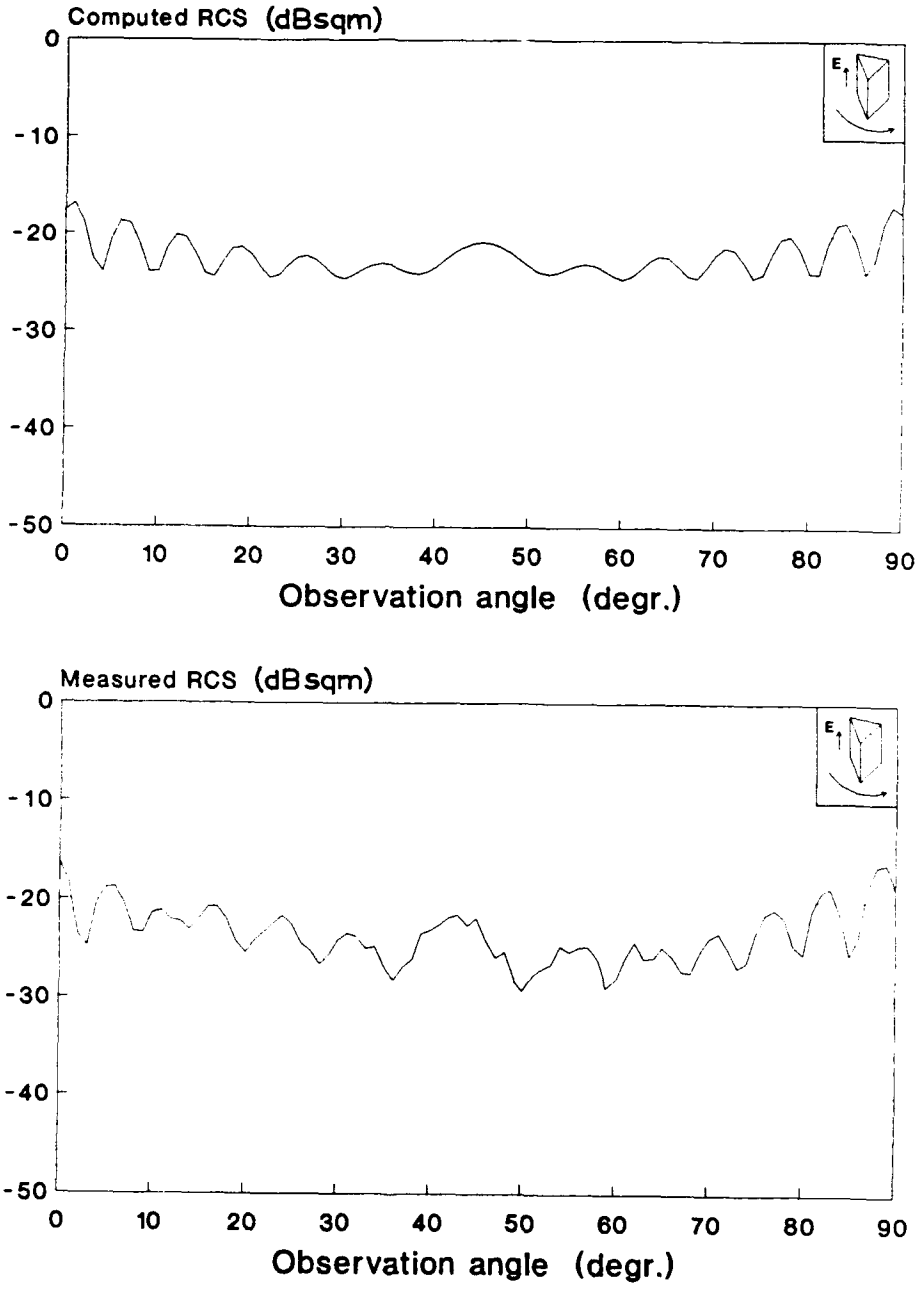

Fig. 42: Computed and measured RCS of Wedge45 at 17 GHz and vertical polarization.

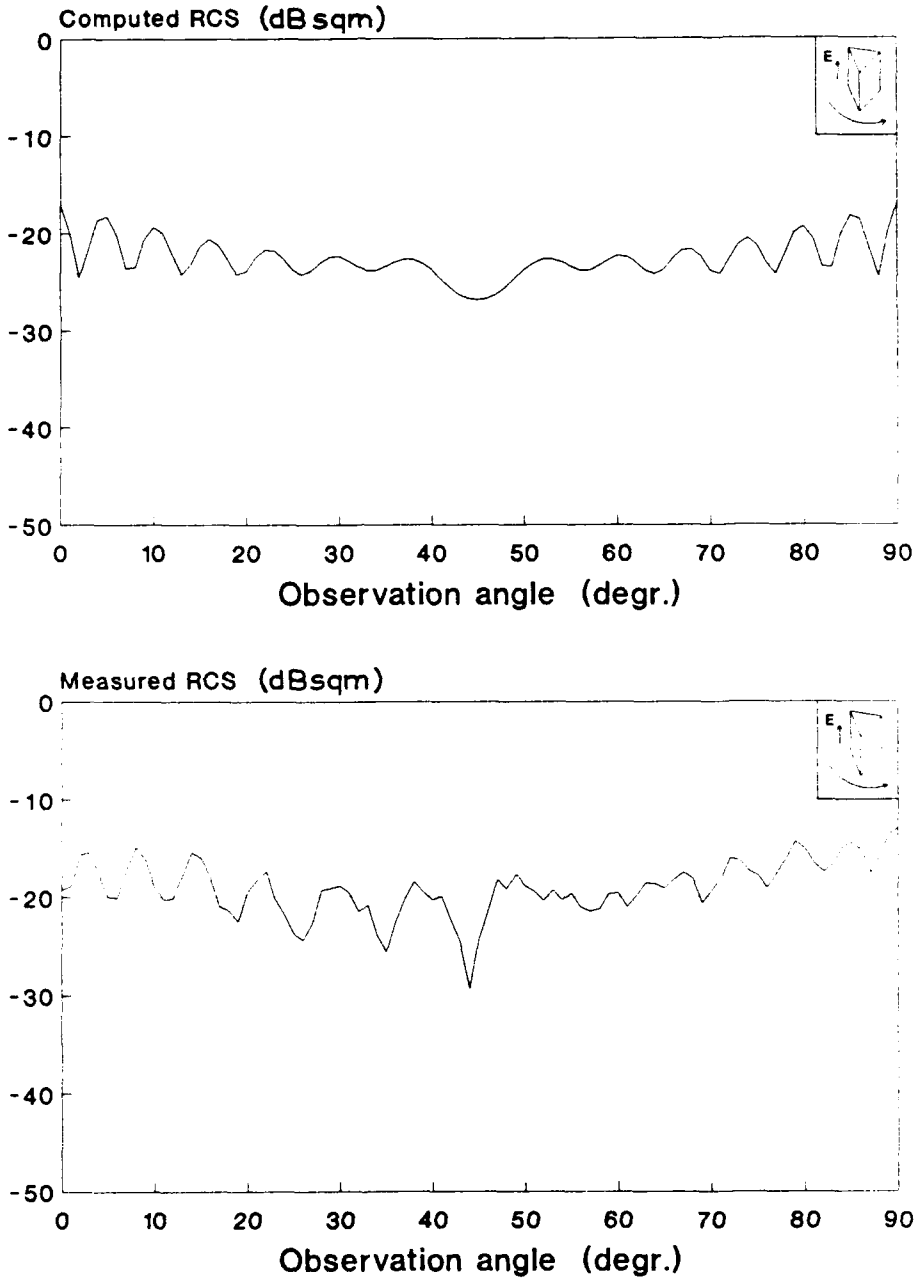

Fig. 43: Computed and measured RCS of Wedge45 at 18 GHz and vertical polarization.

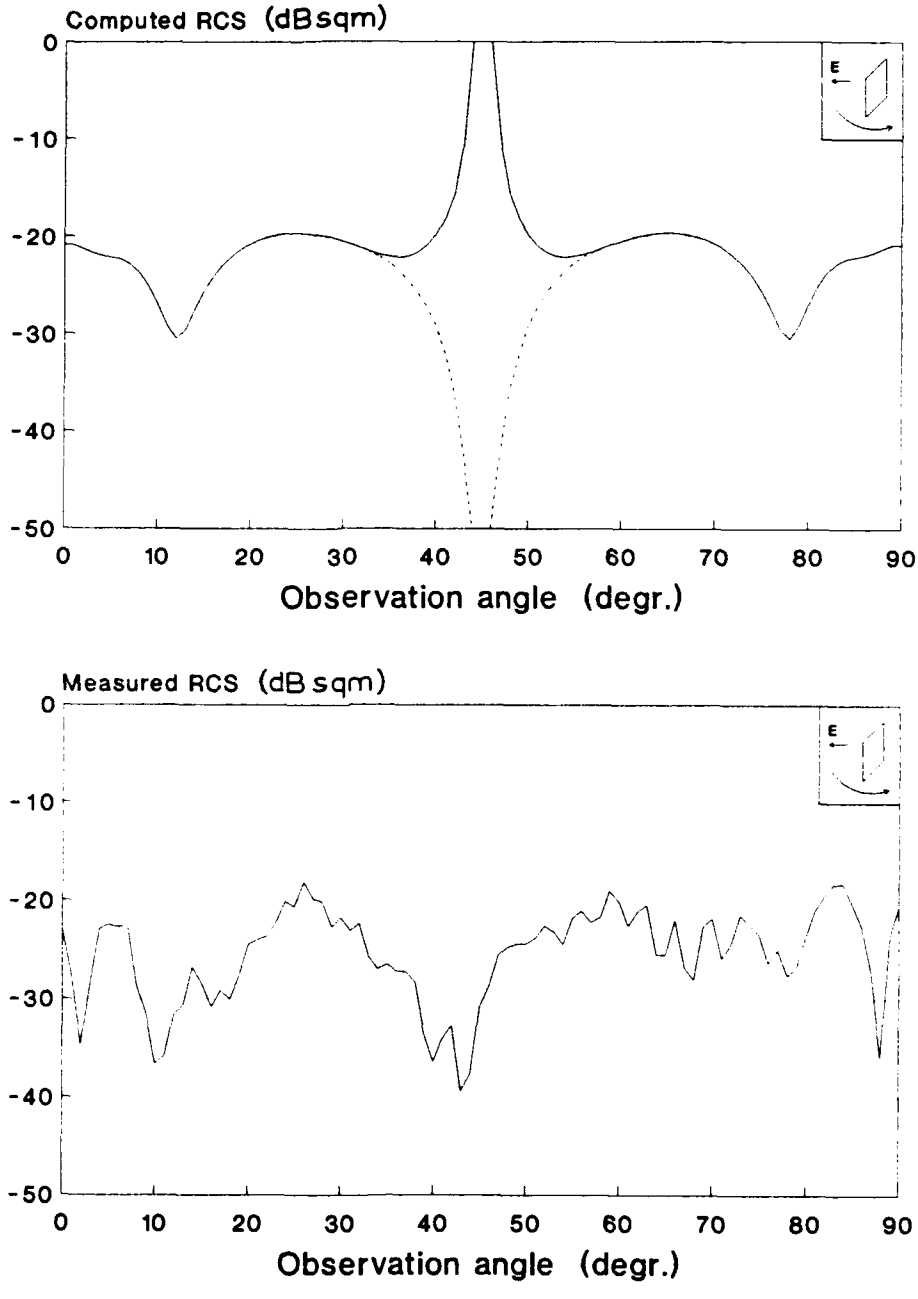

Fig. 44: Newly computed and measured RCS of the plate at 16 GHz and horizontal polarization. Note: the dashed line indicates the expected shape of the curve.

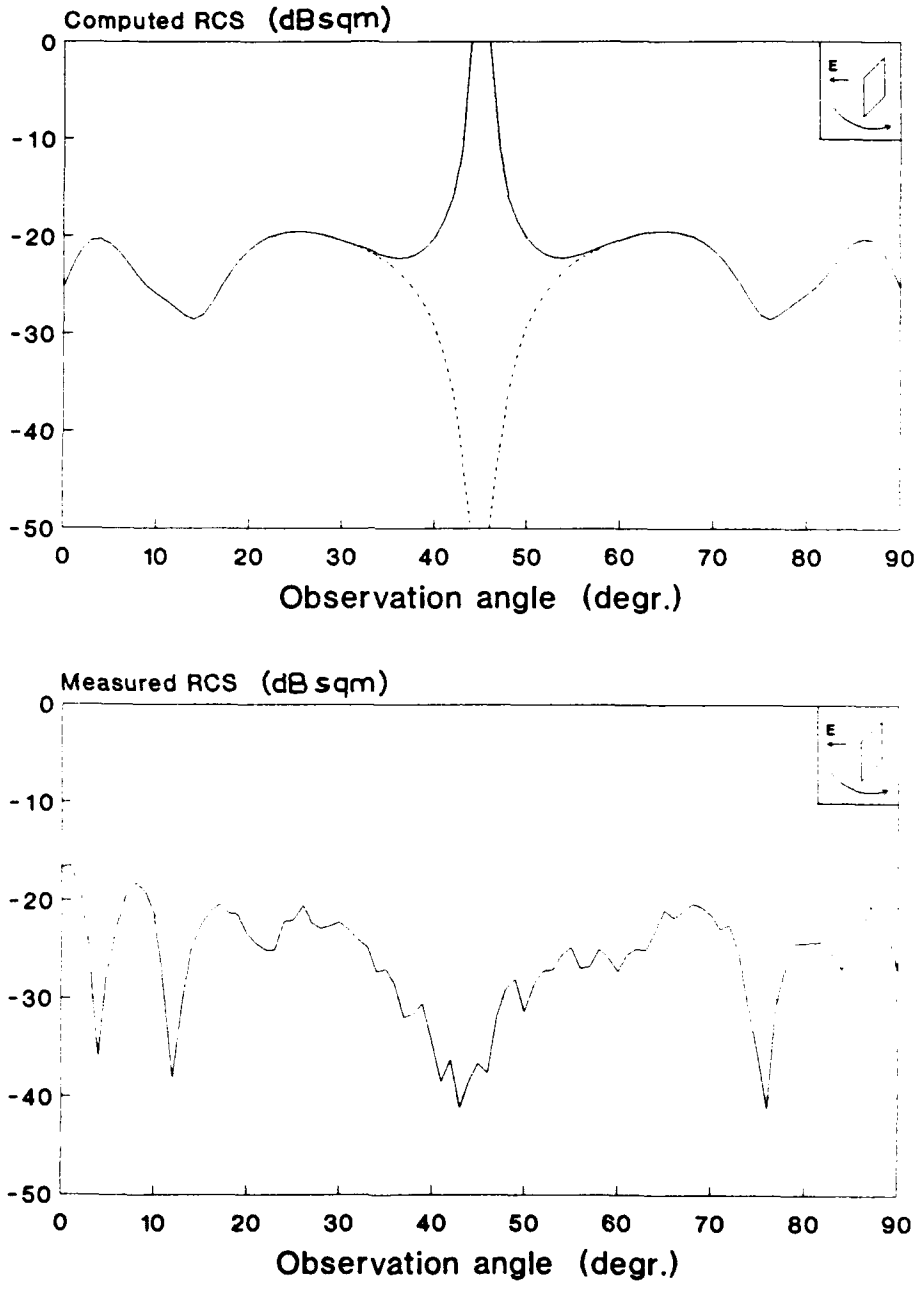

Fig. 45: Newly computed and measured RCS of the plate at 17 GHz and horizontal polarization. Note: the dashed line indicates the expected shape of the curve.

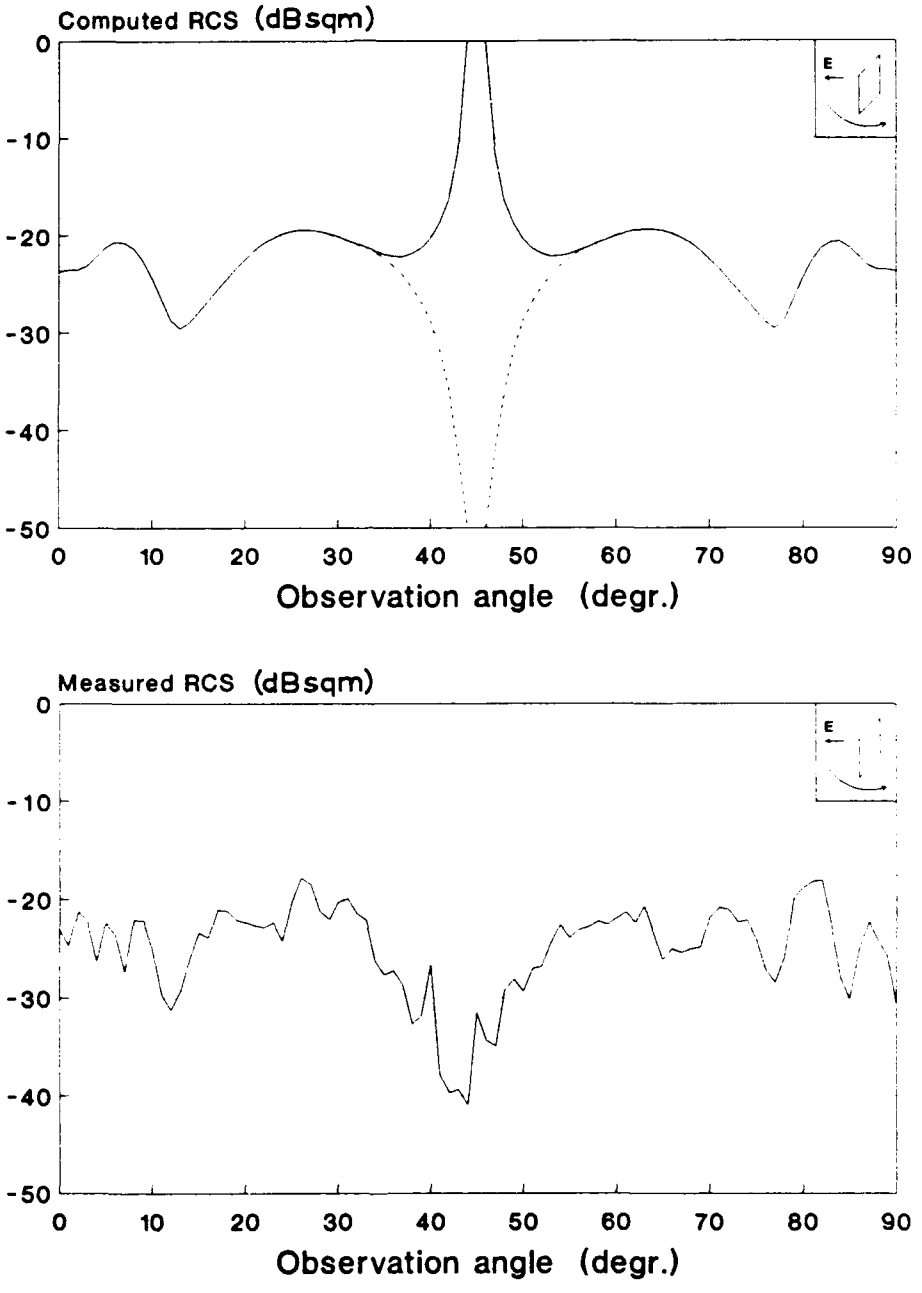

Fig. 46: Newly computed and measured RCS of the plate at 18 GHz and horizontal polarization. Note: the dashed line indicates the expected shape of the curve.

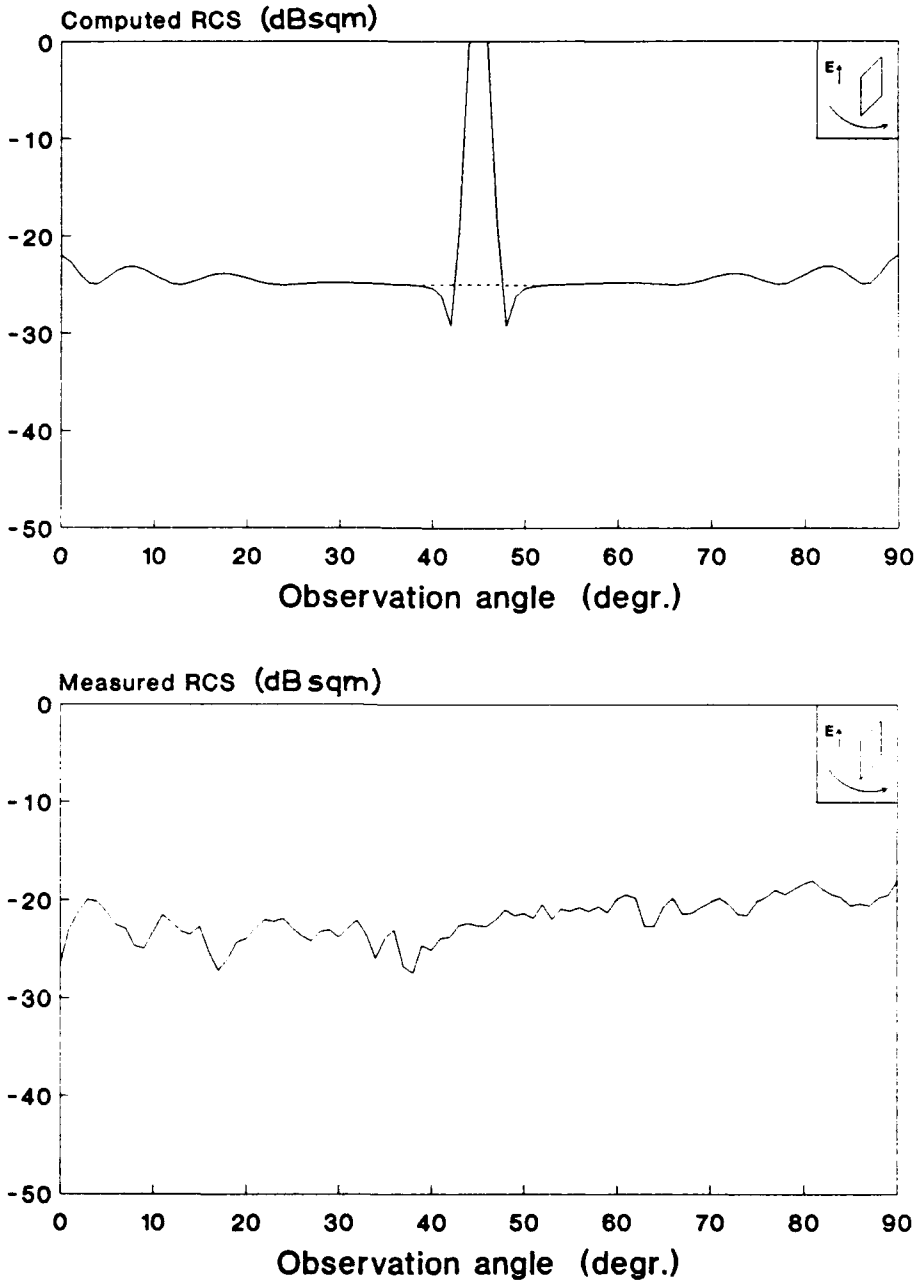

Fig. 47: Newly computed and measured RCS of the plate at 16 GHz and vertical polarization. Note: the dashed line indicates the expected shape of the curve.

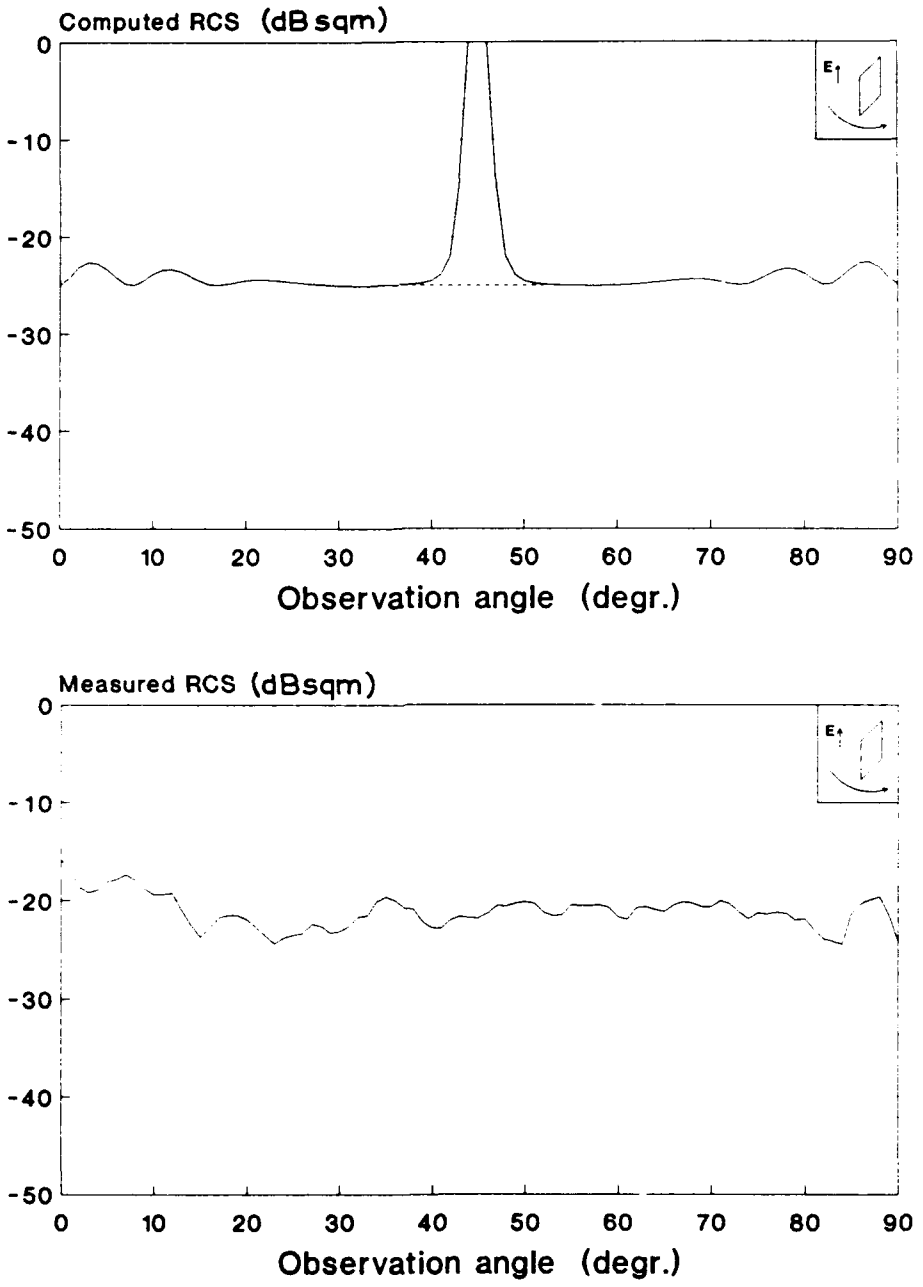

Fig. 48: Newly computed and measured RCS of the plate at 17 GHz and vertical polarization. Note: the dashed line indicates the expected shape of the curve.

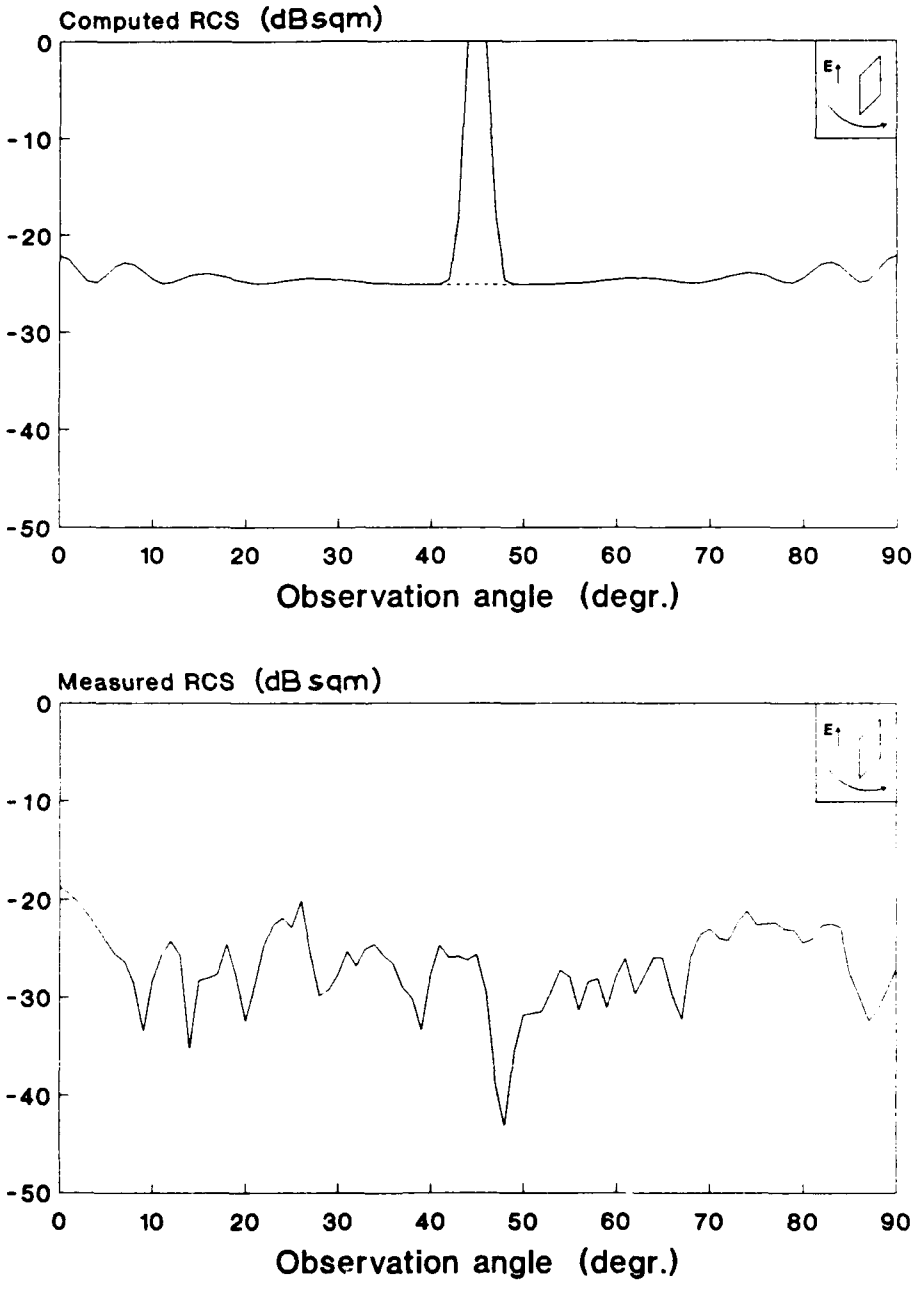

Fig. 49: Newly computed and measured RCS of the plate at 18 GHz and vertical polarization. Note: the dashed line indicates the expected shape of the curve.

5 REFERENCES

[1] Janssen, G.J.M., Hulst, R. vd, Nennie, F.A.: *RCS reduction techniques for square trihedral cone reflectors at 35 GHz, measurements and theoretical simulations*, FEL 1988-04, maart 1988

[2] Wit, M.G.M. de: *"Diffraction theory"*, Physics & Electronics Laboratory TNO, Report to be published.

[3] Hulst, R. van de; Wit, M.G.M. de: *"ANAL2.F program"*, FEL-TNO, undocumented.

[4] Hulst, R. van de: *"MATERIALS datafile"*, FEL-TNO, undocumented.

[5] Hulst, R. van de: *"SCARCE.F program"*, FEL-TNO, undocumented.

[6] Tieman, T.C.B.: *"HPDOS.EXE program"*, FEL-TNO, undocumented.

[7] Ross, R.A.: *"Radar Cross Section of Rectangular Flat Plates as a Function of Aspect Angle"*, IEEE transactions on antennas and propagation, Vol.AP-14 No. 3, May 1966.

[8] Bowman, J.J.; Senior, T.B.A.; Uslenghi, P.L.E.: *"Electromagnetic and Acoustic Scattering by Simple Shapes"*, Section 4.1 and 4.2, North-Holland Publishing Company - Amsterdam, 1969

[9] Shore, Robert A.; Yaghjian, Arthur D.: *"Incremental Diffraction Coefficients for Planar Surfaces"*, IEEE transactions on antennas and propagation, Vol.36, No.1, January 1988.

Ir. G.A. van der Spek
(Group leader)

Ir. J.F.A. Koppelmans
(Author)

LISTINGS OF OBJECT AND PARAMETER FILES

Object file CORNER

```
corner                                                  {name of object}
        3                                               {# polygons of object}
   -0.09175520     0.90824336    -0.40825844            {normal first polygon}
        1                                               {material first polygon}
        3                                               {# corners first polygon}
    0.00638600     0.00638600     0.02841400            {coordinates first corner}
    0.03480000     0.03480000     0.08524000            {coordinates second corner}
    0.06960000     0.00000000     0.00000000            {coordinates third corner}
    0.40824831     0.40824831     0.81649661            {normal second polygon}
        1                                               {material second polygon}
        3                                               {# corners second polygon}
    0.00638600     0.00638600     0.02841400            {coordinates first corner}
    0.06960000     0.00000000     0.00000000            {coordinates second corner}
    0.00000000     0.06960000     0.00000000            {coordinates third corner}
    0.90824336    -0.09175520    -0.40825844            {normal third polygon}
        1                                               {material third polygon}
        3                                               {# corners third polygon}
    0.00638600     0.00638600     0.02841400            {coordinates first corner}
    0.00000000     0.06960000     0.00000000            {coordinates second corner}
    0.03480000     0.03480000     0.08524000            {coordinates third corner}
```

Object file PLATE

```
plate
        1
    0.70710677    -0.70710677     0.00000000
        1
        4
    0.00000000     0.00000000     0.00000000
    0.07071068     0.07071068     0.00000000
    0.07071068     0.07071068     0.10000000
    0.00000000     0.00000000     0.10000000
```

Object file WG05

```
wg05
         3
    0.73727733   -0.67559022    0.00000000
         1
         4
    0.00616871    0.00000000    0.00000000
    0.07372773    0.07372773    0.00000000
    0.07372773    0.07372773    0.10000000
    0.00616871    0.00000000    0.10000000
   -0.67559022    0.73727733    0.00000000
         1
         4
    0.00000000    0.00616871    0.00000000
    0.00000000    0.00616871    0.10000000
    0.07372773    0.07372773    0.10000000
    0.07372773    0.07372773    0.00000000
   -0.70710677   -0.70710677    0.00000000
         1
         4
    0.00616871    0.00000000    0.00000000
    0.00616871    0.00000000    0.10000000
    0.00000000    0.00616871    0.10000000
    0.00000000    0.00616871    0.00000000
```

Object file WG10

```
wg10
         3
    0.76604444   -0.64278764    0.00000000
         1
         4
    0.01232568    0.00000000    0.00000000
    0.07660444    0.07660444    0.00000000
    0.07660444    0.07660444    0.10000000
    0.01232568    0.00000000    0.10000000
   -0.64278764    0.76604444    0.00000000
         1
         4
    0.00000000    0.01232568    0.00000000
    0.00000000    0.01232568    0.10000000
    0.07660444    0.07660444    0.10000000
    0.07660444    0.07660444    0.00000000
   -0.70710677   -0.70710677    0.00000000
         1
         4
    0.01232568    0.00000000    0.00000000
    0.01232568    0.00000000    0.10000000
    0.00000000    0.01232568    0.10000000
    0.00000000    0.01232568    0.00000000
```

Object file WG20

```
wg20
         3
     0.81915206    -0.57357645     0.00000000
         1
         4
     0.02455756     0.00000000     0.00000000
     0.08191520     0.08191520     0.00000000
     0.08191520     0.08191520     0.10000000
     0.02455756     0.00000000     0.10000000
    -0.57357645     0.81915206     0.00000000
         1
         4
     0.00000000     0.02455756     0.00000000
     0.00000000     0.02455756     0.10000000
     0.08191520     0.08191520     0.10000000
     0.08191520     0.08191520     0.00000000
    -0.70710677    -0.70710677     0.00000000
         1
         4
     0.02455756     0.00000000     0.00000000
     0.02455756     0.00000000     0.10000000
     0.00000000     0.02455756     0.10000000
     0.00000000     0.02455756     0.00000000
```

Object file WG45

```
wg45
         3
     0.92387956    -0.38268343     0.00000000
         1
         4
     0.05411961     0.00000000     0.00000000
     0.09238795     0.09238795     0.00000000
     0.09238795     0.09238795     0.10000000
     0.05411961     0.00000000     0.10000000
    -0.38268343     0.92387956     0.00000000
         1
         4
     0.00000000     0.05411961     0.00000000
     0.00000000     0.05411961     0.10000000
     0.09238795     0.09238795     0.10000000
     0.09238795     0.09238795     0.00000000
    -0.70710677    -0.70710677     0.00000000
         1
         4
     0.05411961     0.00000000     0.00000000
     0.05411961     0.00000000     0.10000000
     0.00000000     0.05411961     0.10000000
     0.00000000     0.05411961     0.00000000
```

Parameter file H16

```
h16                     {name of parameter file}
   1                    {simulation type (RCS as function of phi)}
    0.0000              {start point simulation (phi = 0°)}
   90.0000              {stop point simulation (phi = 90°)}
    1.0000              {step (1°)}
    0.0000              {phi (discarded in this case)}
   90.0000              {theta}
   16.0000              {frequency (GHz)}
    0.0000              {bistatic angle dphi}
    0.0000              {bistatic angle dtheta}
horizontaal             {transmitter polarization}
horizontaal             {receiver polarization}
```

Parameter file H17

```
h17
   1
    0.0000
   90.0000
    1.0000
    0.0000
   90.0000
   17.0000
    0.0000
    0.0000
horizontaal
horizontaal
```

Parameter file H18

```
h18
   1
    0.0000
   90.0000
    1.0000
    0.0000
   90.0000
   18.0000
    0.0000
    0.0000
horizontaal
horizontaal
```

Parameter file V16

```
v16
   1
    0.0000
   90.0000
    1.0000
    0.0000
   90.0000
   16.0000
    0.0000
    0.0000
verticaal
verticaal
```

Parameter file V17

```
v17
   1
    0.0000
   90.0000
    1.0000
    0.0000
   90.0000
   17.0000
    0.0000
    0.0000
verticaal
verticaal
```

Parameter file V18

```
v18
   1
    0.0000
   90.0000
    1.0000
    0.0000
   90.0000
   18.0000
    0.0000
    0.0000
verticaal
verticaal
```

UNCLASSIFIED

REPORT DOCUMENTATION PAGE (MOD-NL)

1. DEFENSE REPORT NUMBER (MOD-NL)	2. RECIPIENT'S ACCESSION NUMBER	3. PERFORMING ORGANIZATION REPORT NUMBER
TD91-0983		FEL-91-B043
4. PROJECT/TASK/WORK UNIT NO.	**5. CONTRACT NUMBER**	**6. REPORT DATE**
20369	-	APRIL 1991
7. NUMBER OF PAGES	**8. NUMBER OF REFERENCES**	**9. TYPE OF REPORT AND DATES COVERED**
69 (INCL APP., EXCL. RDP & DISTR.LIST)	9	FINAL

10. TITLE AND SUBTITLE
VALIDATION OF DIFRRACTION THEORY BY MEANS OF EXTENSIVE MEASUREMENTS, PART 1.

11. AUTHOR(S)
IR. J.F.A. KOPPELMANS

12. PERFORMING ORGANIZATION NAME(S) AND ADDRESS(ES)
TNO PHYSICS AND ELECTRONICS LABORATORY, P.O. BOX 96864, 2509 JG THE HAGUE
OUDE WAALSDORPERWEG 63, THE HAGUE, THE NETHERLANDS

13. SPONSORING/MONITORING AGENCY NAME(S)
TNO PHYSICS AND ELECTRONICS LABORATORY, THE HAGUE, THE NETHERLANDS

14. SUPPLEMENTARY NOTES

15. ABSTRACT (MAXIMUM 200 WORDS, 1044 POSITIONS)
IN THE FEL COMPUTER MODEL THE RADAR CROSS SECTION OF ARBITRARY OBJECTS IS CALCULATED BY APPLYING GEOMETRICAL OPTICS AND PHYSICAL OPTICS. IN ORDER TO PERFORM THE COMPUTATIONS MORE ACCURATELY, THE MODEL ALSO ACCOUNTS FOR DIFFRACTION PHENOMENA. THIS REPORT PRESENTS A LARGE NUMBER OF MEASUREMENTS AND SIMULATIONS CARRIED OUT TO VALIDATE THE DIFFRACTION THEORY IMPLEMENTED.
DURING THE ANALYSIS OF THE RESULTS, IT TURNED OUT THAT THERE WAS A LARGE DIFFERENCE BETWEEN MEASUREMENTS USING HORIZONTAL POLARIZATION AND THOSE USING VERTICAL POLARIZATION. AT VERTICAL POLARIZATION THE MEASUREMENTS AND SIMULATIONS GENERALLY SHOWED GOOD AGREEMENT. AT HORIZONTAL POLARIZATION, HOWEVER, LARGE DIFFERENCES BETWEEN THE MEASUREMENTS AND THE SIMULATIONS OCCURRED. FURTHER ANALYSIS SHOWED THAT THESE DIFFERENCES WERE MOST LIKELY DUE TO THE FACT THAT THE IMPLEMENTED DIFFRACTION THEORY DOES NOT ACCOUNT FOR MULTIPLE DIFFRACTION. APART FROM THAT, THE ANECHOIC CHAMBER CAUSED PROBLEMS BECAUSE OF ITS RELATIVELY HIGH "CLUTTER LEVEL", WHICH WAS IN THE SAME ORDER OF MAGNITUDE AS THE MEASURED SIGNALS. FOR FURTHER VALIDATION EFFORTS, IT IS THEREFORE RECOMMENDED TO INCLUDE MULTIPLE DIFFRACTION IN THE COMPUTER MODEL AND TO PERFORM NEW MEASUREMENTS UNDER BETTER CONTROLLED CIRCUMSTANCES.

16. DESCRIPTORS	IDENTIFIERS
RADAR CROSS SECTION	DIFFRACTION
ELECTROMAGNETIC WAVES	PHYSICAL OPTICS
MATHEMATICAL MODEL	
COMPUTATION	
MEASUREMENT	
COMPUTERIZED SIMULATION	

17a. SECURITY CLASSIFICATION (OF REPORT)	17b. SECURITY CLASSIFICATION (OF PAGE)	17c. SECURITY CLASSIFICATION (OF ABSTRACT)
UNCLASSIFIED	UNCLASSIFIED	UNCLASSIFIED

18. DISTRIBUTION/AVAILABILITY STATEMENT
UNLIMITED AVAILABILITY

17d. SECURITY CLASSIFICATION (OF TITLES)
UNCLASSIFIED

UNCLASSIFIED

Distributielijst

1.	Hoofddirecteur van de Hoofdgroep Defensieonderzoek TNO
2.	Directeur Wetenschappelijk Onderzoek en Ontwikkeling
3.	HWO-KL
4.	
t/m	HWO-KLu
5.	
6.	HWO-KM
7.	
t/m	Hoofd TDCK
9.	
10.	Directie FEL-TNO, t.a.v. Ir. P. Spohr
11.	Directie FEL-TNO, t.a.v. Dr. J.W. Maas, daarna reserve
12.	Archief FEL-TNO, in bruikleen aan Ir. G.H. Heebels
13.	Archief FEL-TNO, in bruikleen aan Ir. G.A. van der Spek
14.	Archief FEL-TNO, in bruikleen aan Ir. H.J.M. Heemskerk
15.	Archief FEL-TNO, in bruikleen aan Ir. L.J. van Ewijk
16.	Archief FEL-TNO, in bruikleen aan Dr. M. Brand
17.	Archief FEL-TNO, in bruikleen aan Drs. M. Vogel
18.	Archief FEL-TNO, in bruikleen aan Ir. J.F.A. Koppelmans
19.	Documentatie FEL-TNO
20.	
t/m	Reserves
21.	

Indien binnen de krijgsmacht extra exemplaren van dit rapport worden gewenst door personen of instanties die niet op de verzendlijst voorkomen, dan dienen deze aangevraagd te worden bij het betreffende Hoofd Wetenschappelijk Onderzoek of, indien het een K-opdracht betreft, bij de Directeur Wetenschappelijk Onderzoek en Ontwikkeling.